Chapter 7
Non-Linearly Variable Thickness Disks

7.1 General Differential Equations and Variable Thickness Profile Geometry

The topic discussed here goes well beyond those normally addressed in courses on mechanical design. However, it is advisable to provide complete coverage of the mathematical basics of the method for integrating the differential equations that govern the displacement field of rotating disks whose thickness varies according to a two-parameter linear function, and thus make it possible to determine their stress and strain states. With this approach, which is a generalization of the conical disk problem covered in the preceding Chapter (the conical disk can be obtained as a particular case of this non-linearly variable thickness disk), we can analyse disk profile configurations of undoubted design interest.

The theory presented here can be used to solve any problem involving a disk whose thickness varies according to relation (7.1), with developments entailing the same degree of complexity found in Chap. 6 for the conical disk. From the standpoint of the analytical developments and the complexity of the calculations involved, it is advisable to use this approach where strictly necessary (convergent and/or divergent solid disks with concave and/or convex profile, convergent annular disks with convex profile, divergent annular disks with concave profile) for which, from the purely technical point of view, *secundum non datur*!

When dealing with (Fig. 4.1a) annular disks with divergent conical profile, tapered disks with concave profile, or divergent disks with convex profile, it is advisable to use Stodola's relations (4.1) or (4.2), which characterize the hyperbolic disk. In fact, once the disk's radii r_i and r_e have been established together with the corresponding thicknesses h_i and h_e, it will almost always be possible – with the exceptions indicated in Chap. 4 – to find a value of exponent a appearing in relations (4.1) and (4.2), with which the profile geometry can be correctly

V. Vullo and F. Vivio, *Rotors: Stress Analysis and Design*,
Mechanical Engineering Series, DOI 10.1007/978-88-470-2562-2_7,

described. It will thus be possible to proceed much more simply on the basis of the hyperbolic disk theory, which as we have seen makes it possible to arrive at closed form solutions for the differential equations governing the displacement field.

The disks analysed here are characterized by a non-linearly variation of thickness with the radius expressed by a power of a two-parameter linear function according to relation (7.1), also used by other researchers (see, for example, Güven [32]). As will be discussed below, this relation can define the geometry of a fourfold infinity of profiles, including convergent and divergent conical profiles; the only profiles that cannot be simulated are those with an inflection point, such as uniform strength disks. This family of variable thickness disks was investigated in the elastic field by Eraslan and Argeşo [14] as part of a study addressing the limit angular velocity where, consequently, the rotor is stressed beyond the elastic limit.

Here it is assumed that the disk always has a plane of symmetry perpendicular to the axis, which bisects the thickness, and that the thickness variation function $h = h(r) = h(\rho) = h(t)$ has any one of the following equivalent expressions:

$$h = h_0 \cdot (1 - m \cdot r)^k = h_0 \cdot (1 - n \cdot \rho)^k = h_0 \cdot (1 - t)^k, \tag{7.1}$$

where: h_0 is the thickness at the axis of the disk (which is real for the solid disk and fictitious for the annular disk); r_e is the outer radius; R, for the profiles of interest to us here (see below) is the distance of the axis from apex V (the term apex is used here even if the disk does not feature a pointed tip, e.g., in convex profiles – Fig. 7.1d) where the two symmetrical sides of the profile intersect (Fig. 7.1a, c, d); m, $n = m{\cdot}r_e$ and k are constant geometrical parameters, r is the radius; $\rho = r/r_e$ and $t = r/R = n{\cdot}\rho$ are dimensionless radii relative to r_e and R respectively. The domains of variables ρ and t are $0 \le \rho \le 1$ and $0 \le t \le n$ for solid disks, and $\beta = r_i/r_e \le \rho \le 1$ and $r_i/R \le t \le n$ for annular disks respectively, r_i being the inner radius. The two domains coincide only for disks profiled in order to feature nil thickness at radius r_e (in this case $n = 1$).

By carefully selecting parameters k and m (and therefore n), the above functions can be used to describe a fourfold infinity of disk profiles. Indeed, with function $h = h(\rho)$ we have:

- For $k = 0$, with any value of n, and for $n = 0$, with any value of k, the disk shows constant thickness (see profiles shown with a horizontal dashed line in Fig. 7.1a–d);
- For $k = 1$ and $0 < n < 1$, the disk shows a converging conical profile (Fig. 7.1a), with no limitations for $0 < n{\cdot}\rho \le 1$ (with $n = 1$, the conical disk ends with a pointed tip at the apex, i.e., for $r_e = R$ and $\rho = 1$); also for $k = 1$ and $n > 1$, we have the limitation $0 \le \rho \le 1/n$ (if the disk outer radius r_e is a design datum, such profiles have no physical meaning); again for $k = 1$, but with $n < 0$, the disk shows a diverging conical profile (Fig. 7.1a), with no limitations;
- For $k < 0$, the disk profile is always concave ($d^2h/d\rho^2 > 0$), but with $n < 0$ ($dh/d\rho < 0$), the disk is always converging, whereas with $n > 0$ ($dh/d\rho > 0$) the

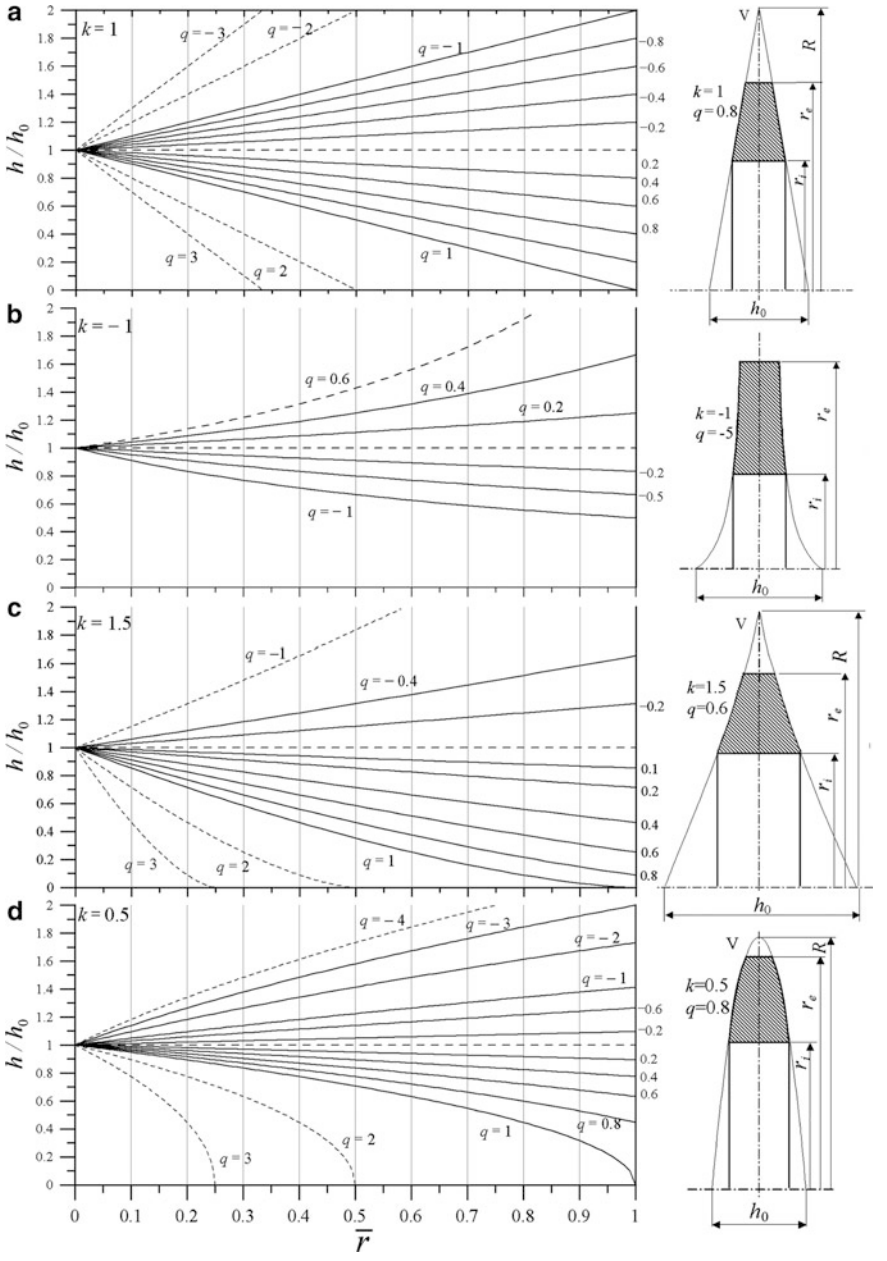

Fig. 7.1 Profiles of solid or annular non-linearly variable thickness disks: (**a**) converging and diverging conical disk ($k = 1$ and positive and negative n); (**b**) converging and diverging concave disk ($k < 0$ and positive and negative n); (**c**) converging and diverging concave disk ($k > 1$ and positive and negative n); (**d**) converging and diverging convex disk ($0 < k < 1$ and positive and negative n)

disk is always diverging, though with a limitation, for $n > 1$, $0 \leq \rho \leq 1/n$ (Fig. 7.1b shows several profiles for $k = -1$ and different values of n);

- For $k > 1$, the disk profile is always concave ($d^2h/d\rho^2 > 0$), but with $n < 0$ ($dh/d\rho > 0$) the disk is always diverging, whereas with $n > 0$ the disk is converging ($dh/d\rho < 0$), though with a limitation, for $n > 1$, $0 \leq \rho \leq 1/n$ (Fig. 7.1c shows several profiles for $k = 1.5$ and different values of n);
- For $0 < k < 1$, the disk profile is always convex ($d^2h/d\rho^2 < 0$), but with $n < 0$ ($dh/d\rho > 0$) the disk is always diverging, whereas with $n > 0$ the disk is converging ($dh/d\rho < 0$), though with a limitation, for $n > 1$, $0 \leq \rho \leq 1/n$ (Fig. 7.1d shows several profiles for $k = 0.5$ and different values of n);
- For $n = -1$ and $k = a$, we have the generalized Stodola disk whose profile, as indicated in Sect. 1.3 and in note 2 to Sect. 3.1, is defined by the relation $h = h_0 \cdot (1 + \rho)^a$ and which, unlike the Stodola profile in the strict sense as given by relations (4.2) or (4.3), does not show a singularity at the axis;
- For $n \to \infty$ e $k \cong a$, we have the true Stodola disk. Bearing in mind (7.1) written in terms of variable ρ together with (4.2) and establishing that the inner, mean and outer radii r_i, r_m and r_e coincide with the corresponding thicknesses h_i, h_m and h_e, we obtain three equalities from which the following relations can be obtained (Calderale et al., 2012):

$$\frac{\ln \beta}{\ln \rho_m} = \frac{\ln\left(\frac{1-n\beta}{1-n}\right)}{\ln\left(\frac{1-n\rho_m}{1-n}\right)}; \quad k = \frac{a \ln \beta}{\ln\left(\frac{1-n\rho_m}{1-n}\right)}; \quad h_0 = \frac{h_e}{(1-n)^k}. \tag{7.2}$$

Solved in succession, these relations make it possible to calculate n, k and h_0. Solved iteratively, the first relation (7.2) gives very high values for the modulus of parameter n, tending to infinity. Thus, the limit for $n \to \infty$ for the second member of the first relation (7.2) is $\ln \beta / \ln \rho_m$. Consequently, the second relation (7.2) yields $k \cong a$, as the limit for $n \to \infty$ of the denominator is $\ln \beta$. The third relation (7.2) then gives $h_0 = \infty$, confirming the singularity of the hyperbola at the disk's rotational axis.

The same conclusions are reached if thickness functions h = h(r) and h = h(t) are considered. As Manna [47] noted for only rotating disks, if we set $t = (r/R)^{2/q} = (n\rho)^{2/q}$in the last relation (7.1), the family of disk profiles that can be analysed can be extended to include, as shown in Fig. 7.2, those with an inflection point, such as uniform strength disks, as well as those that have geometrical singularities at radius R (zero thickness or infinite thickness). The following treatment applies equally to the profile defined by a power of a linear function and a power of a nonlinear function. For the latter, in the relations written in terms of t, we will have $t = (r/R)^{2/q} = (n\rho)^{2/q}$ rather than $t = r/R = n\rho$, while in the relations written in terms of ρ, we will have $\rho = (1/n)t^{q/2}$ instead of $\rho = t/n$.

The terms converging (tapered is a synonym) and diverging are used here to express thickness variation from the axis (or the inner radius) to the outer

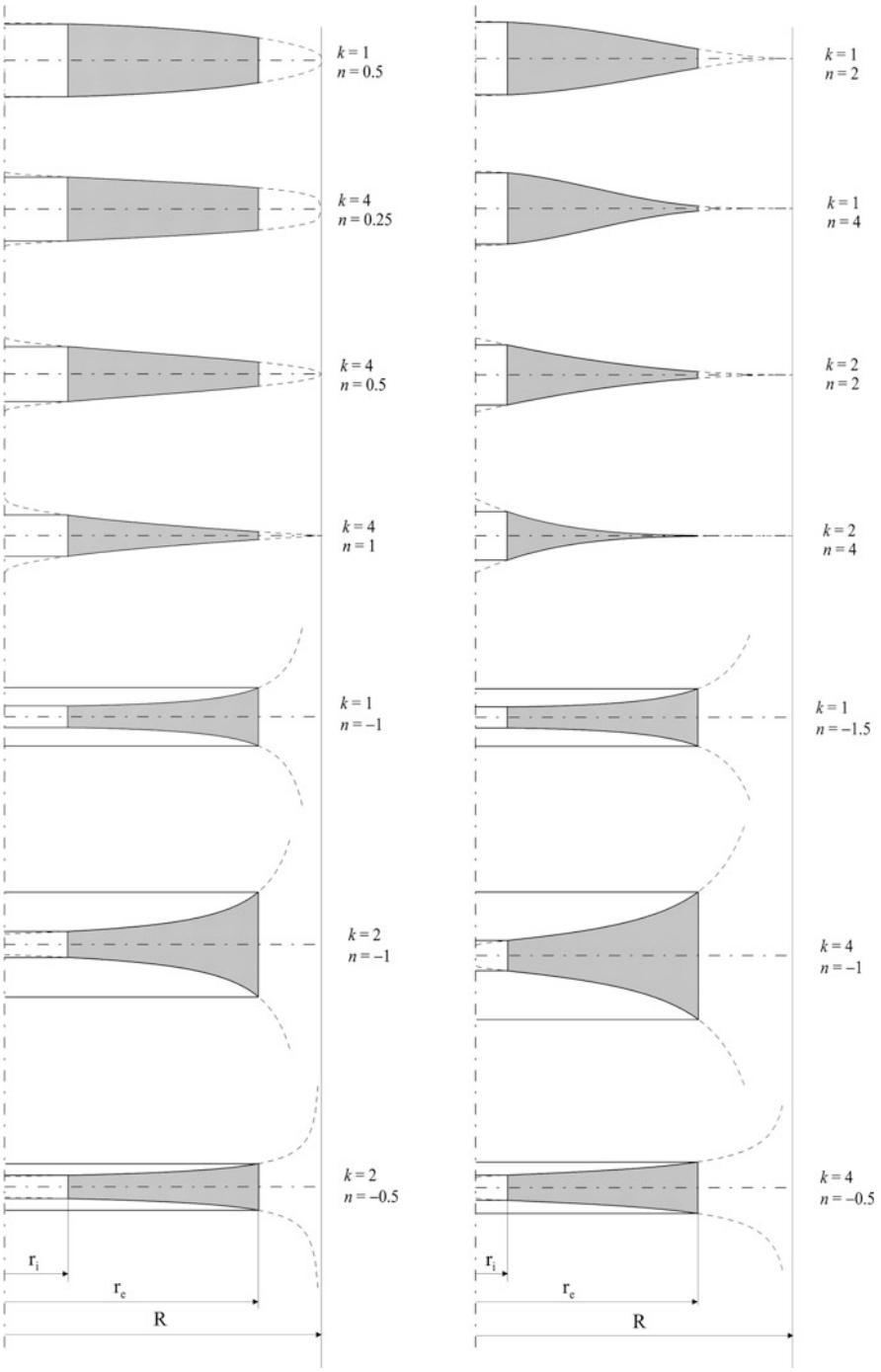

Fig. 7.2 Various profiles of solid or annular non-linear variable thickness disks according to (7.1) and with $t = (r/R)^{2/q} = (n\rho)^{2/q}$

radius. From the application standpoint, interest is limited to converging disks, given that diverging disks, with their unfavourable rotating mass distribution, involve high rotational inertia and equally unfavourable stress and strain states. For manufacturing and design reasons (and, above all, because of functional requirements for current turbine disks, where the axial dimensions of the surface coupling with the shaft must be limited in order to control vibration behaviour for any given distance between bearings), the ratio h_0/h_e must be lower than, or at the most equal to, 3 and thickness h_0 at the axis must not be higher than $(0.25 \div 0.30)r_e$. The outer radius r_e is also a design datum.

Accordingly, considering the values r_e, h_0 and h_e as design data, and selecting the exponent k so as to outline the actual disk profile as closely as possible, the value of n is univocally defined. In fact, $n = 1 - (h_e/h_0)^{1/k}$ at the outer radius, where $\rho = 1$ and $h = h_e$, given function $h = h(\rho)$. This shows that any higher value of n determines profiles of no physical meaning (see non-horizontal dashed profiles in Fig. 7.1). From an even more general viewpoint, by accepting slight variations for r_e, h_0 and h_e from design data, both parameters n and k may be varied, provided that the geometrical relationships between the quantities in relation (7.1) are respected.

As usual, dimensionless radius ρ will be taken into consideration in order to determine the disk size, given that r_e is a design datum. However, because the solution of the homogeneous differential equation entails hypergeometric series in terms of the variable $t = n{\cdot}\rho$, the more general dimensionless radius t will be considered for analytical development. Function $h = h(\rho)$ shows that the local value ρ_V of variable ρ at apex V (Fig. 7.1a, c, d) where, for converging disks, the two symmetrical surfaces of the profile meet, must necessarily be $\rho_V = R/r_e = 1/n$, given that at V the disk shows null thickness. Therefore, $R = r_e/n$ so that, shifting from variable ρ to variable t and considering that $n = m{\cdot}r_e$, then $m{\cdot}R = 1$, whereas the local value of t at radius r_e, where $\rho = 1$, will be $t = r_e/R = n$. Consequently, for converging profiles showing $0 \le h_e/h_0 \le 1$, domain definitions of n and t corresponding to $0 \le \rho \le 1$ are $0 \le n \le 1$ and $0 \le t \le n$ respectively. In this connection, it can be readily seen that, for $t = n$, then $\rho = 1$, whereas for $t = 1$, then $\rho = 1/n$ and $r = R$.

Figure 7.1b shows that a converging concave profile can be obtained from (7.1) by assuming negative values for both n and k. In this case, as will be seen later, of the two independent integrals of the associated homogeneous equation of the differential equation governing the displacement field, the first u_1 is defined in the interval $0 \le \rho \le 1/n$, whereas the second u_2 is defined in the interval $-1/n \le \rho \le 0$, so that neither is usable. Consequently, we will not consider disk profiles obtained from (7.1) showing negative values for n and k: values for which the radius R can only be defined conventionally. This, however, is not a limitation of the proposed procedure, given that, as shown in Fig. 7.2d, converging concave profiles can also be obtained with $0 < k < 1$ and $0 < n < 1$ respectively.

To deduce the differential equation that governs the general displacement field, whatever the configuration of these profiles of the non-linearly variable thickness disk, the expression of h given by (7.1) in terms of variable ρ, is introduced in (1.28) together with its first derivative with respect to ρ, taking into account that

$d/dr = (1/r_e)\cdot d/d\rho$, $d^2/dr^2 = (1/r_e{}^2)\cdot d^2/d\rho^2$, $dh/d\rho = -n\cdot h_0\cdot k\cdot(1 - n\cdot\rho)^{k-1}$ and $(1/h)\cdot(dh/d\rho) = -n\cdot k/(1 - n\cdot\rho)$. We thus obtain the following general solving differential equation of the non-linearly variable thickness rotating disk according to relation (7.1), subjected to thermal load with the generic temperature variation function $T = T(r)$:

$$\frac{d^2u}{d\rho^2}+\left(\frac{1}{\rho}-\frac{n\cdot k}{1-n\cdot\rho}\right)\cdot\frac{du}{d\rho}-\left[\frac{1}{\rho^2}+\frac{v\cdot n\cdot k}{\rho\cdot(1-n\cdot\rho)}\right]\cdot u-(1+v)\cdot\alpha\cdot r_e\cdot \left(\frac{dT}{d\rho}-\frac{n\cdot k\cdot T}{1-n\cdot\rho}\right)+\frac{(1-v^2)\cdot\gamma\cdot\omega^2\cdot r_e^3\cdot\rho}{E}=0. \tag{7.3}$$

For cases in which the disk is subjected only to centrifugal load or only to thermal load, this equation specializes in the following relations:

$$\frac{d^2u}{d\rho^2}+\left(\frac{1}{\rho}-\frac{n\cdot k}{1-n\cdot\rho}\right)\cdot\frac{du}{d\rho}-\left[\frac{1}{\rho^2}+\frac{v\cdot n\cdot k}{\rho\cdot(1-n\cdot\rho)}\right]\cdot u+\frac{(1-v^2)\cdot\gamma\cdot\omega^2\cdot r_e^3\cdot\rho}{E}=0; \tag{7.4}$$

$$\frac{d^2u}{d\rho^2}+\left(\frac{1}{\rho}-\frac{n\cdot k}{1-n\cdot\rho}\right)\cdot\frac{du}{d\rho}-\left[\frac{1}{\rho^2}+\frac{v\cdot n\cdot k}{\rho\cdot(1-n\cdot\rho)}\right]\times u-(1+v)\cdot\alpha\cdot r_e\cdot\left(\frac{dT}{d\rho}-\frac{n\cdot k\cdot T}{1-n\cdot\rho}\right)=0. \tag{7.5}$$

General solutions of the above three non-homogeneous differential equations are obtained by adding the solution of the common associated homogeneous equation to particular solutions of the same complete equations.

$$\frac{d^2u}{d\rho^2}+\left(\frac{1}{\rho}-\frac{n\cdot k}{1-n\cdot\rho}\right)\cdot\frac{du}{d\rho}-\left[\frac{1}{\rho^2}+\frac{v\cdot n\cdot k}{\rho\cdot(1-n\cdot\rho)}\right]\cdot u=0. \tag{7.6}$$

Like (6.6), (7.6) is also a differential equation with coefficients that are analytical functions of the independent variable ρ; it can also be considered as a Fuchs class equation and, being characterized by three singular points ($\rho = 0$; $\rho = 1/n$, $\rho = \infty$), is the classic Gauss hypergeometric differential equation. Equation 7.6 makes it possible to treat both Stodola's hyperbolic disk and its generalization as particular cases. For the former, bearing in mind that the limits for $n \to \infty$ (here, we consider n in modulus) of ratios $-nk/(1 - n\rho)$ and $-vnk/[\rho(1 - n\rho)]$ appearing in (7.6) are k/ρ and $-vk/\rho^2$ respectively, and noting that $k \cong a$, it is clear that this equation reduces to the homogeneous equation associated with equations (4.4) and (4.7), as well as to (4.11). For the generalization of the hyperbolic disk, differential equation (7.6) must be rewritten in terms of $n = -1$ and $k = a$.

7.2 Rotating Disk Having Constant Density

As indicated above, the differential equation that governs the displacement field when the disk is subjected only to centrifugal load is (7.4), whose solution is the sum of the associated homogeneous equation, given by (7.6), and a particular integral of the complete equation.

7.2.1 Particular Integral and Corresponding Stress and Strain State

To obtain the particular integral of Eq. 7.4, it is best to start from (1.28) without thermal load. The following non-homogeneous differential equation is obtained by introducing the thickness function (7.1) in terms of the variable r in (1.28) together with its first derivative with respect to r, and introducing the notation (6.8):

$$\frac{d^2u}{dr^2}+\left(\frac{1}{r}-\frac{m\cdot k}{1-m\cdot r}\right)\cdot\frac{du}{dr}-\left[\frac{1}{r^2}+\frac{v\cdot m\cdot k}{r\cdot(1-m\cdot r)}\right]\cdot u=-C\cdot r. \tag{7.7}$$

To obtain the particular integral u_p of differential equation (7.7), we put

$$u_p=c_1\cdot r+c_2\cdot r^2+c_3\cdot r^3, \tag{7.8}$$

where c_1, c_2 and c_3 are constants that can be determined by substituting (7.8), along with its first and second derivatives with respect to variable r, in (7.7), and by equating to zero the coefficients of various powers in the variable r. We thus obtain:

$$c_1=\frac{3\cdot(3+v)\cdot C}{m^2\cdot(1+v)\cdot[8+k\cdot(3+v)]\cdot[3+k\cdot(2+v)]};$$

$$c_2=\frac{k\cdot(3+v)\cdot C}{m\cdot[8+k\cdot(3+v)]\cdot[3+k\cdot(2+v)]};\ c_3=-\frac{C}{8+k\cdot(3+v)}. \tag{7.9}$$

By substituting (7.9) in (7.8), bearing in mind the notation (6.8), which expresses C and by changing from variable r to ρ, we obtain:

$$u_p=-\frac{(1-v^2)}{[8+k\cdot(3+v)]}\cdot\rho \cdot\left\{\rho^2-\frac{3+v}{[3+k\cdot(2+v)]}\cdot\left[\frac{k\cdot\rho}{n}+\frac{3}{n^2\cdot(1+v)}\right]\right\}\cdot\gamma\cdot\frac{\omega^2\cdot r_e^3}{E}. \tag{7.10}$$

However, in the usual assumptions of small displacements and plane stress ($\sigma_z = 0$) made for disks (thickness small by respect to the outer radius r_e), radial and hoop stresses are given by relations (1.27). Consequently, the following stress state correlated to particular integral u_p is obtained by substituting (7.10) and its derivative $du_p/d\rho$, after changing from variable r to variable ρ, bearing in mind that $r = r_e \cdot \rho$ and $du_p/dr = (1/r_e) \cdot (du_p/d\rho)$ in relations (1.27), from which temperature terms are omitted:

$$\begin{cases} \sigma_r = -\gamma \cdot \omega^2 \cdot r_e^2 \cdot g_r = \sigma_0 \cdot g_r \\ \sigma_t = -\gamma \cdot \omega^2 \cdot r_e^2 \cdot g_t = \sigma_0 \cdot g_t, \end{cases} \tag{7.11}$$

where $\sigma_0 = \gamma \cdot \omega^2 \cdot {r_e}^2$ is the reference stress and g_r and g_t are dimensionless functions of ρ v, k and n, given respectively by:

$$\begin{cases} g_r = -\dfrac{1}{[8 + k \cdot (3 + v)]} \\ \quad \times \left[(3 + v) \cdot \rho^2 - \dfrac{(2 + v) \cdot (3 + v)}{[3 + k \cdot (2 + v)]} \cdot \dfrac{k}{n} \cdot \rho - \dfrac{3 \cdot (3 + v)}{[3 + k \cdot (2 + v)] \cdot n^2} \right] \\ g_t = -\dfrac{1}{[8 + k \cdot (3 + v)]} \\ \quad \times \left[(1 + 3v) \cdot \rho^2 - \dfrac{(1 + 2v) \cdot (3 + v)}{[3 + k \cdot (2 + v)]} \cdot \dfrac{k}{n} \cdot \rho - \dfrac{3 \cdot (3 + v)}{[3 + k \cdot (2 + v)] \cdot n^2} \right]. \end{cases} \tag{7.12}$$

It should be noted that relations (7.12), where t is substituted for ρ, are generalizations of (6.14), obtained for the conical disk, which is thus a specific case of the non-linearly variable-thickness disk. These relations can be used to obtain, for $n = k = 1$, relations for the converging conical disk, and for $n = -1$ and $k = 1$ relations for the diverging conical disk (Fig. 7.1a).

It can be concluded from (7.10) that the particular integral u_p, and thus its related stress state given by relations (7.11) and the resulting strain state given by (1.25), from which temperature terms are omitted (after substituting relations (7.11) in them, and bearing (7.12) in mind) largely depend on the disk's material, geometrical dimensions and rotation speed. For any given material, u_p is proportional to ${r_e}^3$ and to ω^2. It should be noted that, for a given disk of assigned geometry (n, k and r_e fixed) and for a specific angular velocity, the structure of (7.10) shows that the particular integral may be defined once and for all: in other words, once the disk geometry is established, u_p can be determined for any other angular velocity by means of a simple scale shift.

Figure 7.3 shows functions g_r and g_t versus ρ, for two steel disks ($v = 0.3$) with $h_0/h_e \cong 3$, one of which has a convex profile ($k = 0.5$ and $n = 0.89$), while the other has a concave profile ($k = 1.5$ and $n = 0.52$). Through σ_0, functions g_r and g_t are proportional to the radial and hoop stresses σ_r and σ_t related to particular integral u_p, which as will be demonstrated below has an inherent physical meaning:

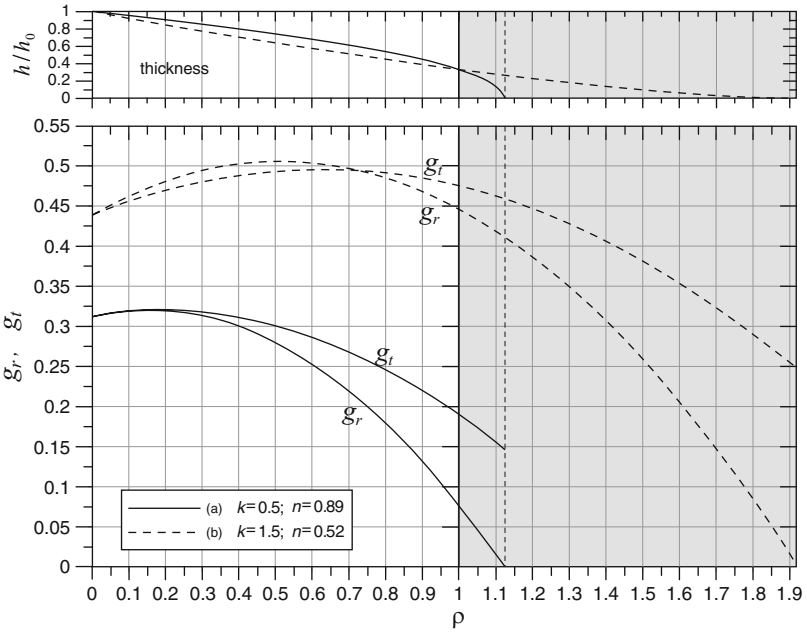

Fig. 7.3 Curves of g_r and g_t as a function of ρ within the interval $0 \leq \rho \leq 1/q$, for two steel disks ($v = 0.3$), with ratio $h_0/h_e \cong 3$ and with variable profile according to (7.1): (*a*) convex profile ($k = 0.5$ and $n = 0.89$); (*b*) concave profile ($k = 1.5$ and $n = 0.52$)

it represents radial displacement in a solid disk whose thickness varies according to a power of a linear function, with concave or convex profile, extended to its apex V where $r = R$ and $\rho = 1/n$. It should be noted that functions g_r and g_t assume finite values throughout the interval $0 \leq \rho \leq 1/n$ ($0 \leq t \leq 1$); only g_r becomes null at the right edge of the interval, i.e., for $\rho = 1/n$ ($t = 1$).

It should also be noted that relations (7.12) are only valid in the interval of the variable ρ showing physical meaning ($0 \leq \rho \leq 1$). To extend their validity from $\rho = 1$ to $\rho = 1/n$, to calculate functions g_r and g_t as well as related stresses, it would be necessary to reconsider the actual value of the outer radius which, in this case, shifts from r_e to R (this entails considering a scale factor equal to n^2). Clearly, the same consideration applies to calculating displacement u_p, as obtained by relation (7.10). For the sake of completeness, the curve of functions g_r and g_t in the interval $1 < \rho \leq 1/n$ is also shown in Figure 7.3, although said scale factor should be considered for calculation purposes. This interval is represented with a dashed line in the figure.

7.2.2 Solution of Homogeneous Differential Equation and Corresponding Stress and Strain State

To solve (7.6), which is the common homogeneous equation associated with the three complete differential equation (7.3), (7.4) and (7.5), it is best to introduce variable $t = n{\cdot}\rho$, whereby, as $d\rho = dt/n$ and $d\rho^2 = dt^2/n^2$, (7.6) becomes:

$$\frac{d^2u}{dt^2} + \left(\frac{1}{t} + \frac{k}{t-1}\right) \cdot \frac{du}{dt} + \left[\frac{1}{t} + (\nu \cdot k - 1)\right] \cdot \frac{u}{t \cdot (t-1)} = 0. \tag{7.13}$$

Like (6.15), this is a hypergeometric differential equation, showing three singular points ($t = 0$; $t = 1$; $t = \infty$) and corresponding to the general Papperitz form given by (6.16), again with:

$$\alpha + \alpha' + \beta + \beta' + \gamma + \gamma' = 1. \tag{7.14}$$

The following relations can be deduced from a comparison of (7.13) with (6.16), taking (7.14) into account:

$$\begin{gathered} 1 - \alpha - \alpha' = 1;\ \ 1 - \gamma - \gamma' = k;\ \ \beta \cdot \beta' = \nu \cdot k - 1; -\alpha \cdot \alpha' = 1; \\ \gamma \cdot \gamma' = 0;\ \ \beta + \beta' = k \end{gathered} \tag{7.15}$$

Consequently, for the case examined here we obtain:

$$\begin{gathered} \alpha = -1;\ \ \alpha' = 1;\ \ \gamma = 1 - k;\ \ \gamma' = 0;\ \ \beta = \frac{k}{2} + \xi;\ \ \beta' = \frac{k}{2} - \xi; \\ \text{with } \xi = \frac{1}{2} \cdot \sqrt{k^2 + 4 \cdot (1 - \nu \cdot k)}. \end{gathered} \tag{7.16}$$

According to the general theory mentioned in Sect. 6.2.2, (7.13), which is equivalent to (6.16), allows for two independent integrals, chosen from the four given by relations (6.20). However, in the case examined here, and taking (7.16) into account, relations (6.20) become:

$$\begin{aligned} u_1 &= t \cdot (1-t)^{1-k} \cdot F\left(2 - \frac{k}{2} + \xi, 2 - \frac{k}{2} - \xi, 3, t\right) \\ u_{1'} &= t \cdot F\left(1 + \frac{k}{2} + \xi, 1 + \frac{k}{2} - \xi, 3, t\right) \\ u_2 &= t^{-1} \cdot (1-t)^{1-k} \cdot F\left(-\frac{k}{2} + \xi,\ -\frac{k}{2} - \xi,\ -1, t\right) \\ u_{2'} &= t^{-1} \cdot F\left(-1 + \frac{k}{2} + \xi,\ -1 + \frac{k}{2} - \xi,\ -1, t\right). \end{aligned} \tag{7.17}$$

For convergence, the same considerations made for relations (6.21) also apply here.

In this context, it is necessary to select as the first integral of (7.13) the one deriving from the second relation (7.17), which is here designated u_1 and transcribed as:

$$u_1 = \quad t^{\alpha'} \cdot (1-t)^{\gamma} \cdot F(a,b,c,t) \; = t \cdot F\left(1+\frac{k}{2}+\xi, 1+\frac{k}{2}-\xi, 3, t\right) \tag{7.18}$$

where, for the sake of brevity, the following notation is used:

$$a = \alpha' + \beta + \gamma = 1 + \frac{k}{2} + \xi; \;\; b = \alpha' + \beta' + \gamma = 1 + \frac{k}{2} - \xi; \;\; c = 1 + \alpha' - \alpha = 3, \tag{7.19}$$

whereas $F(a, b, c, t)$ indicates the infinite hypergeometric series of the kind (6.24). This hypergeometric series slowly converges for $| t | = | n \cdot \rho | < 1$, which implies $0 < n < 1$. In other words, n is always lower than 1, as the actual disk profile mostly develops in the interval $0 \leq \rho \leq 1$. More specifically, the hypergeometric series $F(a, b, c, t)$ is divergent if the real part $\Re(c - a - b) \leq -1$, absolutely convergent if $\Re(c - a - b) > 0$ and, excluding the singularity point $t = 1$, conditionally convergent if $-1 < \Re(c - a - b) \leq 0$. Here, given that, a, b and c are real coefficients and $(c - a - b) = 1 - k$, for tapered disks, we have divergence for $k \geq 2$, absolute convergence for $0 < k < 1$ and conditional convergence for $1 \leq k < 2$. In the case of convergent disks, the range of variability of parameters n and k featured in (7.1) is thus limited, given that $0 < n < 1$, with $0 < k < 1$ for absolute convergence and $1 \leq n < 2$ for conditional convergence.

Given that the first derivative of the radial displacement $u = u(r)$ must be calculated in order to determine stress and strain states (in this regard, see (1.27) and (1.25)), it should be borne in mind that the first derivative with respect to variable t in series (6.24) is given by relation (6.26).

It is now necessary to find a second integral of differential equation (7.13) which is independent of that given by relation (7.18). In this respect, it should be noted that, here as earlier, the series appearing in the last two relations (7.17), featuring infinite terms from a certain value onwards, actually become finite when the interfering negative integer factors are freely increased by a small quantity ε, which, however, will need to be minimized by multiplying it by a suitable constant coefficient so as to prevent sensible terms from tending to infinity.

Therefore, given that relations (6.27), (6.28), (6.29) and (6.30) are still valid, developing the calculations with respect to the first and third of expressions (7.17) and with the necessary changes with respect to the conical disk (i.e., substituting notations (6.20) for the corresponding notations (6.23)), it can be shown that the following relations apply instead of relations (6.31):

$$\begin{cases} u_1^* = t \cdot F\left(1+\dfrac{k}{2}+\xi, 1+\dfrac{k}{2}-\xi, 3-\varepsilon, t\right) \\ u_2^* = t^{-1+\varepsilon} \cdot F\left(-1+\dfrac{k}{2}+\xi+\varepsilon, -1+\dfrac{k}{2}-\xi+\varepsilon, -1+\varepsilon, t\right) \\ \mathrm{m}(2,\varepsilon) = \dfrac{\varepsilon \cdot (\varepsilon-1)}{\left(\dfrac{k}{2}+\xi+\varepsilon\right) \cdot \left(\dfrac{k}{2}-\xi+\varepsilon\right) \cdot \left(-1+\dfrac{k}{2}+\xi+\varepsilon\right) \cdot \left(-1+\dfrac{k}{2}-\xi+\varepsilon\right)}. \end{cases} \tag{7.20}$$

and that the second independent integral of (7.13) is given by relation:

$$u_2 = \frac{2}{\left(\dfrac{k}{2}+\xi\right) \cdot \left(\dfrac{k}{2}-\xi\right)} \cdot \left[1 - \frac{t^{-1}}{\left(-1+\dfrac{k}{2}+\xi\right) \cdot \left(-1+\dfrac{k}{2}-\xi\right)}\right] + u_1 \cdot \ln\ t + t \cdot \sum_{i=1}^{\infty} C_i \cdot t^i \tag{7.21}$$

with

$$C_i = \frac{\prod_{m=1}^{i} \left(1+\dfrac{k}{2}+\xi+m-1\right) \cdot \left(1+\dfrac{k}{2}-\xi+m-1\right)}{i! \cdot \prod_{m=1}^{i} (3+m-1)} \cdot \sum_{m=0}^{i-1} \left(\frac{1}{1+\dfrac{k}{2}+\xi+m} + \frac{1}{1+\dfrac{k}{2}-\xi+m} - \frac{1}{1+m} - \frac{1}{3+m}\right). \tag{7.22}$$

Thus, the second independent integral of the hypergeometric differential equation (7.13) is determined. Figure 7.4a, b show the two independent integrals u_1 and u_2 versus ρ within the interval $0 \leq \rho \leq 1/n$ for two convergent disks with profile according to (7.1), the first being a convex disk falling in the range of absolute convergence ($k = 0.5$ and $n = 0.89$), and the second a concave disk falling in the range of conditional convergence ($k = 1.5$ and $n = 0.52$). Here, too, it should be noted that, outside the interval where variable ρ has physical meaning, i.e., for $1 < \rho \leq 1/n$ (see Fig. 7.4a, b, to the right of the vertical dashed line, $\rho = 1$), the scale factor indicated in the previous section must be introduced for calculation purposes. In Fig. 7.4c, the curves of integrals u_1 and u_2 are shown for a concave converging disk for which both parameters n and k are negative ($k = -1$ and $n = -1$); in this case, integral u_2, by contrast with integral u_1, is not defined in

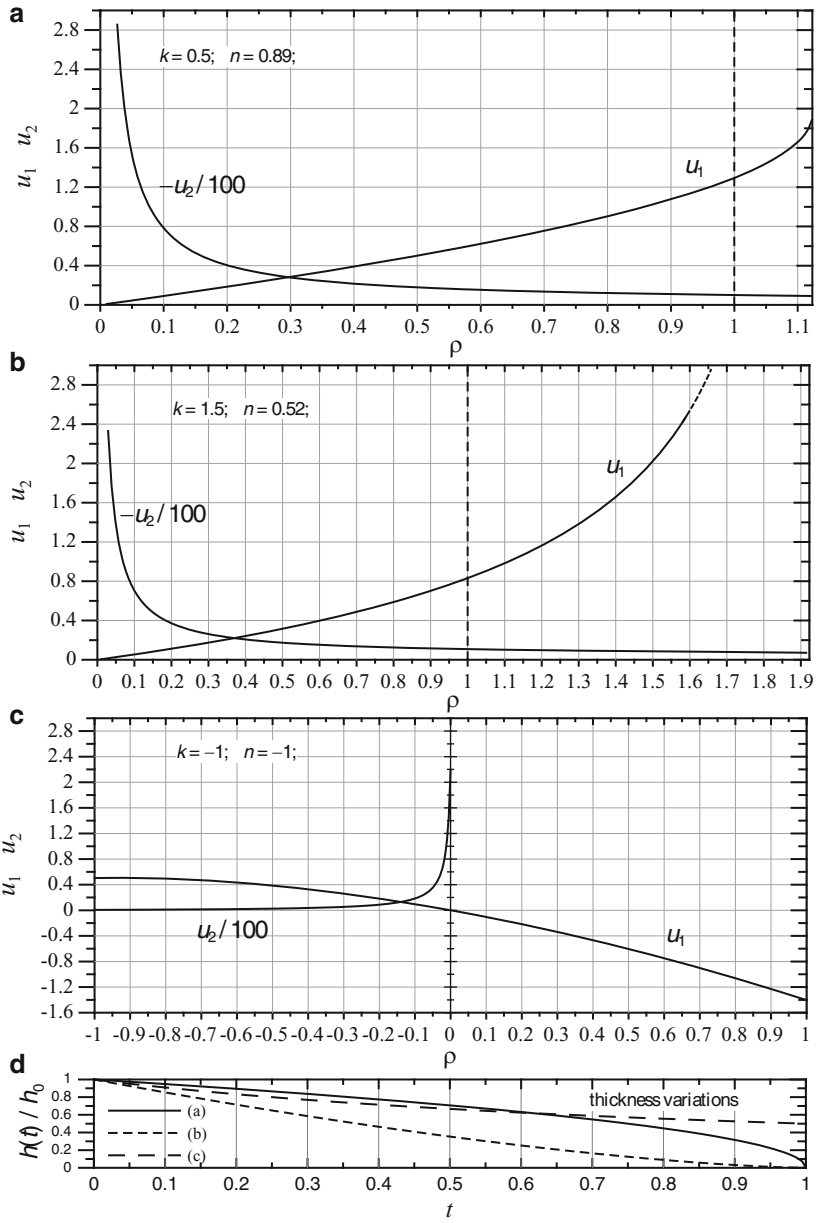

Fig. 7.4 Curves of u_1 and u_2 as a function of ρ, within the interval $0 \leq \rho \leq 1/n$, for three converging steel disks ($\nu = 0.3$) with profile varying according to (7.1): (**a**) convex profile ($k = 0.5$ and $n = 0.89$); (**b**) concave profile ($k = 1.5$ and $n = 0.52$); (**c**) concave profile ($k = -1$ and $n = -1$); (**d**) profiles of the three disk types

the interval $0 \leq \rho \leq 1/n$ considered here, so that it is not usable. However, this does not restrict the generality of this theoretical analysis, given that concave converging profiles (the same can be said for diverging disks, which are of no interest with regard to rotors) can be obtained with $0 < n < 1$ and $1 \leq k < 2$ (Fig. 7.4c), instead of with both n and k negative (Fig. 7.1b).

From Fig. 7.4a, b, as well as from the structure of relations (7.18) and (7.21), while considering (7.22), we can conclude that $u_1 \rightarrow \infty$ for $\rho \rightarrow 1/n$, whereas $u_2 \rightarrow \infty$ for $\rho \rightarrow 0$. It should also be noted that, if the profile at the apex V does not feature a pointed tip, as is the case for convex profiles (Fig. 7.1d), u_1 has a finite value for $\rho = 1/n$, i.e., there is no singularity.

Here, these integrals are used directly in the following developments, as was done for the conical disk (see Sect. 6.2.2). By using the integrals directly, the solution of the associated homogeneous equation (7.13) can be expressed by means of relation (6.34), where C_1 and C_2 are new integration constants that can be evaluated from the boundary conditions.

Subsequently, the following relations are obtained by replacing relation (6.34), written in terms of ρ, and its first derivative, in relations (1.27) from which temperature terms are omitted, and by considering that $d/dr = (1/r_e)d/d\rho$. These relations express σ_r and σ_t as a function of dimensionless radius ρ:

$$\begin{aligned}
\sigma_r &= \frac{E}{r_e \cdot (1 - v^2)} \cdot \left[C_1 \cdot \left(\frac{du_1}{d\rho} + v \cdot \frac{u_1}{\rho} \right) + C_2 \cdot \left(\frac{du_2}{d\rho} + v \cdot \frac{u_2}{\rho} \right) \right] \\
\sigma_t &= \frac{E}{r_e \cdot (1 - v^2)} \cdot \left[C_1 \cdot \left(\frac{u_1}{\rho} + v \cdot \frac{du_1}{d\rho} \right) + C_2 \cdot \left(\frac{u_2}{\rho} + v \cdot \frac{du_2}{d\rho} \right) \right].
\end{aligned} \tag{7.23}$$

These relations can be expressed in the compact form given by (6.36), where, however

$$a_r = \frac{du_1}{d\rho} + v \cdot \frac{u_1}{\rho},\ b_r = \frac{du_2}{d\rho} + v \cdot \frac{u_2}{\rho},\ a_t = \frac{u_1}{\rho} + v \cdot \frac{du_1}{d\rho} \text{ and } b_t = \frac{u_2}{\rho} + v \cdot \frac{du_2}{d\rho} \tag{7.24}$$

are functions of ρ, v, k and n, whereas:

$$A = \frac{E \cdot C_1}{r_e \cdot (1 - v)} \text{ e } B = \frac{E \cdot C_2}{r_e \cdot (1 + v)} \tag{7.25}$$

are the dimensional integration constants, to be determined by imposing boundary conditions. Derivatives $du_1/d\rho$ and $du_2/d\rho$ are obtained by taking relation (6.26), written in terms of ρ, into consideration once functions u_1 and u_2 have been determined. Calculating functions a_r, b_r, a_t and b_t, each of which is related to different hypergeometric functions (u_1 or u_2), presents no difficulties.

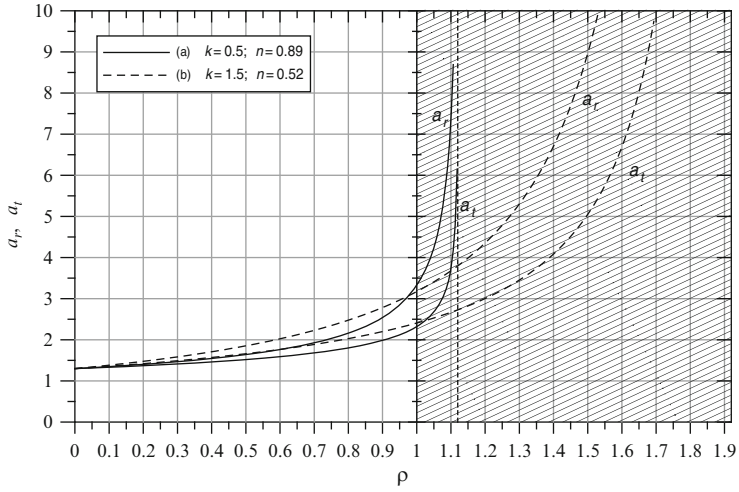

Fig. 7.5 Curves of a_r and a_t as a function of ρ within the interval $0 \leq \rho \leq 1/n$, for two steel disks ($\nu = 0.3$) with profile varying according to (7.1): (*a*) convex profile ($k = 0.5$ and $n = 0.89$); (*b*) concave profile ($k = 1.5$ and $n = 0.52$)

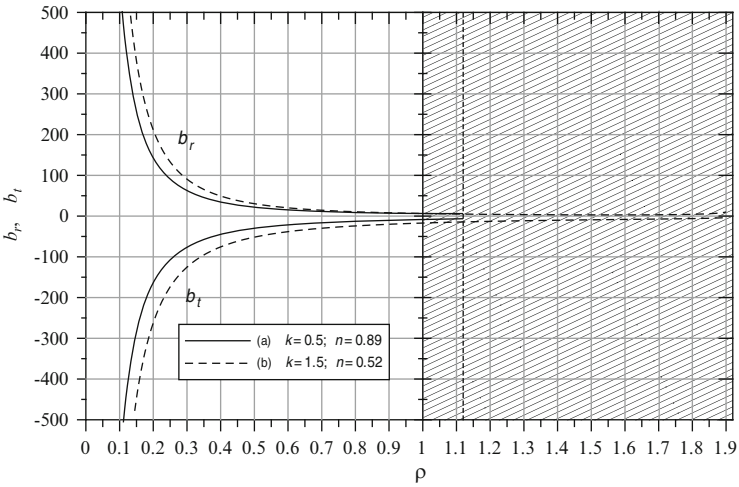

Fig. 7.6 Curves of b_r and b_t as a function of ρ within the interval $0 \leq \rho \leq 1/n$, for two steel disks ($\nu = 0.3$) with profile varying according to (7.1): (*a*) convex profile ($k = 0.5$ and $n = 0.89$); (*b*) concave profile ($k = 1.5$ and $n = 0.52$)

Figures 7.5 and 7.6 show these functions a_r, b_r, a_t and b_t versus dimensionless variable ρ, for both steel disks ($\nu = 0.3$), whose independent integrals u_1 and u_2 are shown in Fig. 7.4a, b respectively. These diagrams make it possible to calculate these functions rapidly for $0 < \rho < 1$, which is the range of variation of ρ for both converging disks of potential technical interest, which may be solid or annular, one

being convex and the other concave. It should be noted that, with the exception of the convex profile, for which a_r, like u_1, has a finite value for $\rho = 1/n$, a_r and a_t tend to infinity for $\rho \to 1/n$ for all other cases of technical interest, given that $u_1 \to \infty$ at the outer edge of the pointed-tip disk ($r = R$, $\rho = 1/n$), whereas b_r and b_t, tend to infinity for $\rho \to 0$, i.e., at the disk axis, given that $u_2 \to \infty$ for $r \to 0$ ($\rho \to 0$).

The strain state related to the stress state given by relations (6.36), written in terms of ρ, is then obtained from (1.25) from which temperature terms are omitted. Radial displacement can then be determined immediately, as $u = r \cdot \varepsilon_t$.

Finally, it should be noted that all of the above relations are generalizations of those obtained for the conical disk, which is thus a specific case of the variable-thickness disk according to (7.1). These relations can be used to obtain, for $n = k = 1$, relations for the converging conical disk, and for $n = -1$ and $k = 1$, relations for the diverging conical disk.

7.2.3 *General Integral and Corresponding Stress and Strain State*

As was specified at the beginning of this paragraph, the general solution of the non-homogeneous differential equation (7.4) governing the displacement field of the rotating disk without thermal load is the sum of the solution of its associated homogeneous equation (7.6), given by (6.34), with u_1 and u_2 given respectively by (7.18) and (7.21), and of the particular integral u_p, previously obtained and given by (7.10). Thus, radial displacement u at the generic dimensionless radius t will be obtained from relation (6.39) written in terms of ρ.

By using the method of superposition in calculating total strains and stresses and by considering relations (7.23) as well as relations (7.11), where g_r and g_t are obtained from relations (7.12), we find that radial and hoop stresses in a rotating disk having variable profile described by means of a power of a linear function, and also subjected to surface force distribution at inner and outer radii, are still expressed by means of relations (6.40), where $\sigma_0 = \gamma \cdot \omega \cdot r_e^2$.

Here again, the strain distributions related to the stress distributions given by (6.40) are obtained from (1.25) from which temperature terms are omitted, after substituting (6.40) in them. We will then have $u = r \cdot \varepsilon_t$.

7.3 Non-Linearly Variable Thickness Disks Having Constant Density and Subjected to Thermal Load

We will now consider a variable thickness disk of constant density and subjected to thermal load only; this disk features a temperature gradient distribution along its radius expressed by relation (4.6) deriving from the function $T = T(r)$ given by (4.5). In this case, passing to variable ρ, the solving differential equation (7.5) becomes:

$$\frac{d^2u}{d\rho^2}+\left(\frac{1}{\rho}-\frac{n\cdot k}{1-n\cdot\rho}\right)\cdot\frac{du}{d\rho}-\left[\frac{1}{\rho^2}+\frac{\nu\cdot n\cdot k}{\rho\cdot(1-n\cdot\rho)}\right]\cdot u-\alpha\cdot(1+\nu)\cdot r_e \cdot\left(\sum_{i=1}^{n} i\cdot k_i\cdot\rho^{i-1}-\frac{n\cdot k}{1-n\cdot\rho}\sum_{i=1}^{n}k_i\cdot\rho^i\right)=0. \tag{7.26}$$

The general integral of this equation is the sum of the solution of the homogeneous equation, which is already known, and of a particular integral of the non-homogeneous equation. Using the superposition method, the latter can be obtained as the linear combination of contributions deriving from component n terms $k_i\cdot\rho^i$ (with $i=1, 2, \ldots, n$, as the constant term k_0 does not contribute to the stress state) of the function $T=T(r)$; thus, by considering the *i-th* term of this function equation (7.26) becomes:

$$\frac{d^2u}{d\rho^2}+\left(\frac{1}{\rho}-\frac{n\cdot k}{1-n\cdot\rho}\right)\cdot\frac{du}{d\rho}-\left[\frac{1}{\rho^2}+\frac{\nu\cdot n\cdot k}{\rho\cdot(1-n\cdot\rho)}\right]\cdot u+\alpha\cdot(1+\nu)\cdot r_e\cdot k_i \cdot\frac{n\cdot(i+k)\cdot\rho^i-i\cdot\rho^{i-1}}{1-n\cdot\rho}=0. \tag{7.27}$$

To obtain a particular integral u'_p of differential eqaution (7.27), we first put

$$u'_p=a_{i+1}\cdot\rho^{i+1}+a_i\cdot\rho^i+a_{i-1}\cdot\rho^{i-1}+\ldots., \tag{7.28}$$

where $a_{i+1}, a_i, a_{i-1}, \ldots.$ are constants; by substituting this relation, along with its first and second derivatives, in (7.27) and by equalling to zero the coefficients of various powers in the variable ρ, the following relations are obtained:

$$a_{i+1}=\alpha\cdot r_e\cdot k_i\cdot\frac{(i+k)\cdot(1+\nu)}{(i+1)\cdot(i+1+k)-(1-\nu\cdot k)}$$
$$a_i=\alpha\cdot r_e\cdot k_i\cdot\frac{i\cdot k\cdot(1-\nu^2)}{n\cdot[i\cdot(i+k)-(1-\nu\cdot k)]\cdot[(i+1)\cdot(i+1+k)-(1-\nu\cdot k)]}, \tag{7.29}$$

while for the subsequent coefficients a_{i-p}, with $p=1, 2, \ldots$, we can derive the general relation

$$a_{i-p}=a_{i-p+1}\cdot\frac{(i-p)\cdot(i-p+2)}{n\cdot[(i-p)\cdot(i-p+k)-(1-\nu\cdot k)]}. \tag{7.30}$$

If we take $i=p$ in relation (7.30), we obtain $a_0=0$. On the basis of the same relation, all coefficients after a_0 related to all negative powers of ρ are thus zero. Therefore, given i as any positive integer, the polynomial (7.28), within the first $(i+1)$ terms starting from the linear term $a_1\cdot\rho$, always represents a particular integral of (7.27).

By substituting the series expansion (7.28) and its first derivative in (1.27), while considering (7.29) and (7.30) as well as the *i-th* term of the function $T = T(r)$, i.e., $T = k_i \cdot \rho^i$, we obtain the following expressions of the corresponding stresses σ_r and σ_t as polynomials of grade i in ρ, with a constant, non-zero term, which are valid for any value of i:

$$\begin{cases} \sigma_r = E \cdot \alpha \cdot k_i \cdot \left(A_i \cdot \rho^i + A_{i-1} \cdot \rho^{i-1} + ... + A_2 \cdot \rho^2 + A_1 \cdot \rho + A_0\right) \\ \quad = E \cdot \alpha \cdot k_i \cdot \varphi_i(\rho) \\ \sigma_t = E \cdot \alpha \cdot k_i \cdot \left(B_i \cdot \rho^i + B_{i-1} \cdot \rho^{i-1} + ... + B_2 \cdot \rho^2 + B_1 \cdot \rho + B_0\right) \\ \quad = E \cdot \alpha \cdot k_i \cdot \psi_i(\rho). \end{cases} \tag{7.31}$$

The coefficients A and B appearing in expressions (7.31) are obtained from the following relations:

$$\begin{aligned} A_i &= -\frac{i}{(i+1)\cdot(i+1+k)-(1-\nu\cdot k)} \\ A_{i-1} &= \frac{k\cdot i\cdot(i+\nu)}{n\cdot[(i+1)\cdot(i+1+k)-(1-\nu\cdot k)]\cdot[i\cdot(i+k)-(1-\nu\cdot k)]} \\ B_i &= -\frac{i\cdot(i+1+k)}{(i+1)\cdot(i+1+k)-(1-\nu\cdot k)} \\ B_{i-1} &= \frac{k\cdot i\cdot(1+\nu\cdot i)}{n\cdot[(i+1)\cdot(i+1+k)-(1-\nu\cdot k)]\cdot[i\cdot(i+k)-(1-\nu\cdot k)]}, \end{aligned} \tag{7.32}$$

while all the subsequent coefficients A_{i-1-p} and B_{i-1-p}, with $p = 1, 2, \ldots, (i-1)$, are derived progressively through the relations:

$$\begin{aligned} A_{i-1-p} &= A_{i-p}\cdot\frac{(i-p+\nu)}{(i-p+1+\nu)}\cdot\frac{(i-p)\cdot(i-p+2)}{n\cdot[(i-p)\cdot(i-p+k)-(1-\nu\cdot k)]} \\ B_{i-1-p} &= B_{i-p}\cdot\frac{1+\nu\cdot(i-p)}{1+\nu\cdot(i-p+1)}\cdot\frac{(i-p)\cdot(i-p+2)}{n\cdot[(i-p)\cdot(i-p+k)-(1-\nu\cdot k)]}, \end{aligned} \tag{7.33}$$

These relations are obtained by means of simple proportions between the coefficients of the powers in ρ^{i-p-1} and ρ^{i-p}. Given that coefficients A_{i-1} and B_{i-1} are known, as directly defined from the second and the fourth expressions (7.32) respectively, relations (7.33) can be used to progressively determine all other coefficients present in (7.31). It can be readily seen that, for a specific value of i, $\sum_{i=0}^{n} A_i = 0$. These relations, in any case, clearly show that coefficients A and B appearing in polynomials $\varphi_i(\rho)$ and $\psi_i(\rho)$, are simply functions of i, ν, k and n.

In general terms, for any value of i, the relations whereby functions $\varphi_i(\rho)$ and $\psi_i(\rho)$ appearing in expression (7.31) can be calculated are as follows

$$\varphi_i(\rho) = -\frac{i\cdot\rho^i}{i^2+2i+k\cdot(1+i+v)} + \frac{i\cdot\prod_{j=2}^{i}(j^2-1)}{n^i\cdot\prod_{j=1}^{i}[j^2+2j+k\cdot(1+j+v)]}$$
$$+ i\cdot\left[\prod_{j=2}^{i}(j^2-1)\right]\cdot\sum_{m=1}^{i-1}\frac{(m+1+v)\cdot k\cdot\rho^m}{n^{i-m}\cdot\left[\prod_{j=1}^{m}(j^2+2j)\right]\cdot\prod_{j=m}^{i}[j^2+2j+k\cdot(1+j+v)]};$$
$$\psi_i(\rho) = -\frac{i\cdot(k+i+1)\cdot\rho^i}{i^2+2i+k\cdot(1+i+v)} + \frac{i\cdot\prod_{j=2}^{i}(j^2-1)}{n^i\cdot\prod_{j=1}^{i}[j^2+2j+k\cdot(1+j+v)]}$$
$$+ i\cdot\left[\prod_{j=2}^{i}(j^2-1)\right]\cdot\sum_{m=1}^{i-1}\frac{[1+(m+1)\cdot v]\cdot k\cdot\rho^m}{n^{i-m}\cdot\left[\prod_{j=1}^{m}(j^2+2j)\right]\cdot\prod_{j=m}^{i}[j^2+2j+k\cdot(1+j+v)]}. \tag{7.34}$$

These general relations derived by the authors [78] can be used to obtain several others of greater technical relevance for engineering calculations, viz.: $i = 1$ (linear variation of temperature with radius); $i = 2$ (temperature variation with radius according to a second-order function); $i = 3$ (temperature variation with radius according to a third-order function). Indeed, almost all functions $T = T(r)$ found in commonly used disks can be satisfactorily approximated with a third-order polynomial. The explicit relations whereby $\varphi_i(\rho)$ and $\psi_i(\rho)$ can be calculated for $i = 1, 2, 3$, are as follows

(a) For $i = 1$, $T = k_1\cdot\rho$ and, hence:

$$\varphi_1(\rho) = \frac{1-n\cdot\rho}{n\cdot[3+k\cdot(2+v)]};\ \psi_1(\rho) = \frac{1-(2+k)\cdot n\cdot\rho}{n\cdot[3+k\cdot(2+v)]}; \tag{7.35}$$

(b) For $i = 2$, $T = k_2\cdot\rho^2$ and, hence:

$$\varphi_2(\rho) = \frac{2\cdot\left\{-n^2\rho^2\cdot[3+k\cdot(2+v)]+(2+v)\cdot n\cdot k\cdot\rho+3\right\}}{n^2\cdot[8+k\cdot(3+v)]\cdot[3+k\cdot(2+v)]};$$
$$\psi_2(\rho) = \frac{2\cdot\left\{-n^2\rho^2\cdot(k+3)\cdot[3+k\cdot(2+v)]+(1+2v)\cdot n\cdot k\cdot\rho+3\right\}}{n^2\cdot[8+k\cdot(3+v)]\cdot[3+k\cdot(2+v)]}; \tag{7.36}$$

(c) For $i = 3$, $T = k_3 \cdot \rho^3$ and, hence:

$$\begin{aligned}\varphi_3(\rho) &= \frac{3\cdot\left\{k\cdot n^2\rho^2\cdot(3+\nu)\cdot[3+k\cdot(2+\nu)]+8\cdot k\cdot n\cdot\rho\cdot(2+\nu)+24\right\}}{n^3\cdot[15+k\cdot(4+\nu)]\cdot[8+k\cdot(3+\nu)]\cdot[3+k\cdot(2+\nu)]}\\ &\quad -\frac{3\cdot\left\{n^3\rho^3\cdot[8+k\cdot(3+\nu)]\cdot[3+k\cdot(2+\nu)]\right\}}{n^3\cdot[15+k\cdot(4+\nu)]\cdot[8+k\cdot(3+\nu)]\cdot[3+k\cdot(2+\nu)]};\\ \psi_3(\rho) &= \frac{3\cdot\left\{k\cdot n^2\rho^2\cdot(1+3\nu)\cdot[3+k\cdot(2+\nu)]+8\cdot k\cdot n\cdot\rho\cdot(1+2\nu)+24\right\}}{n^3\cdot[15+k\cdot(4+\nu)]\cdot[8+k\cdot(3+\nu)]\cdot[3+k\cdot(2+\nu)]}\\ &\quad -\frac{3\cdot\left\{n^3\rho^3\cdot(k+4)\cdot[8+k\cdot(3+\nu)]\cdot[3+k\cdot(2+\nu)]\right\}}{n^3\cdot[15+k\cdot(4+\nu)]\cdot[8+k\cdot(3+\nu)]\cdot[3+k\cdot(2+\nu)]}.\end{aligned} \tag{7.37}$$

Figure 7.7a, b show functions $\varphi_i(\rho)$ and $\psi_i(\rho)$ up to $i = 10$ versus dimensionless variable ρ for two steel disks ($\nu = 0.3$), one convex ($k = 0.5$ and $n = 0.89$), and the other concave ($k = 1.5$ and $n = 0.52$).

On the basis of the foregoing considerations and expressions (6.36) written in terms of ρ, the stress state can be expressed as follows where a non-zero temperature gradient is present along the radius given by relation (4.6):

$$\begin{cases}\sigma_r = A\cdot a_r + B\cdot b_r + E\cdot\alpha\cdot(k_1\cdot\varphi_1 + k_2\cdot\varphi_2 + k_3\cdot\varphi_3 + ...)\\ \quad = A\cdot a_r + B\cdot b_r + E\cdot\alpha\cdot\varphi(\rho)\\ \sigma_t = A\cdot a_t + B\cdot b_t + E\cdot\alpha\cdot(k_1\cdot\psi_1 + k_2\cdot\psi_2 + k_3\cdot\psi_3 + ...)\\ \quad = A\cdot a_t + B\cdot b_t + E\cdot\alpha\cdot\psi(\rho),\end{cases} \tag{7.38}$$

with $\varphi_i = \varphi_i(\rho)$ and $\psi_i = \psi_i(\rho)$.

Here again, the strain state associated with the stress state given by relations (7.38) is obtained from (1.25), after substituting (7.38) in them; we will then have $u = r\cdot\varepsilon_t$.

Here as elsewhere, it should be noted that all of the above relations for thermal load are generalizations of those obtained for the conical disk, which is thus a specific case of the variable-thickness disk according to (7.1). Written in terms of variable t, these relations can be used to obtain, for $n = k = 1$, relations for the converging conical disk, and for $n = -1$ and $k = 1$ relations for the diverging conical disk.

7.4 Non-Linearly Variable Thickness Disks Having Density Variation on Radius

We will now consider a disk having variable profile described by means of a power of a linear function, subjected to centrifugal load and featuring density variation along its radius expressed by the polynomial relation:

$$\gamma = \gamma_0 + \gamma_1\cdot\rho + \gamma_2\cdot\rho^2 + ... = \sum_{i=0}^{n}\gamma_i\cdot\rho^i \tag{7.39}$$

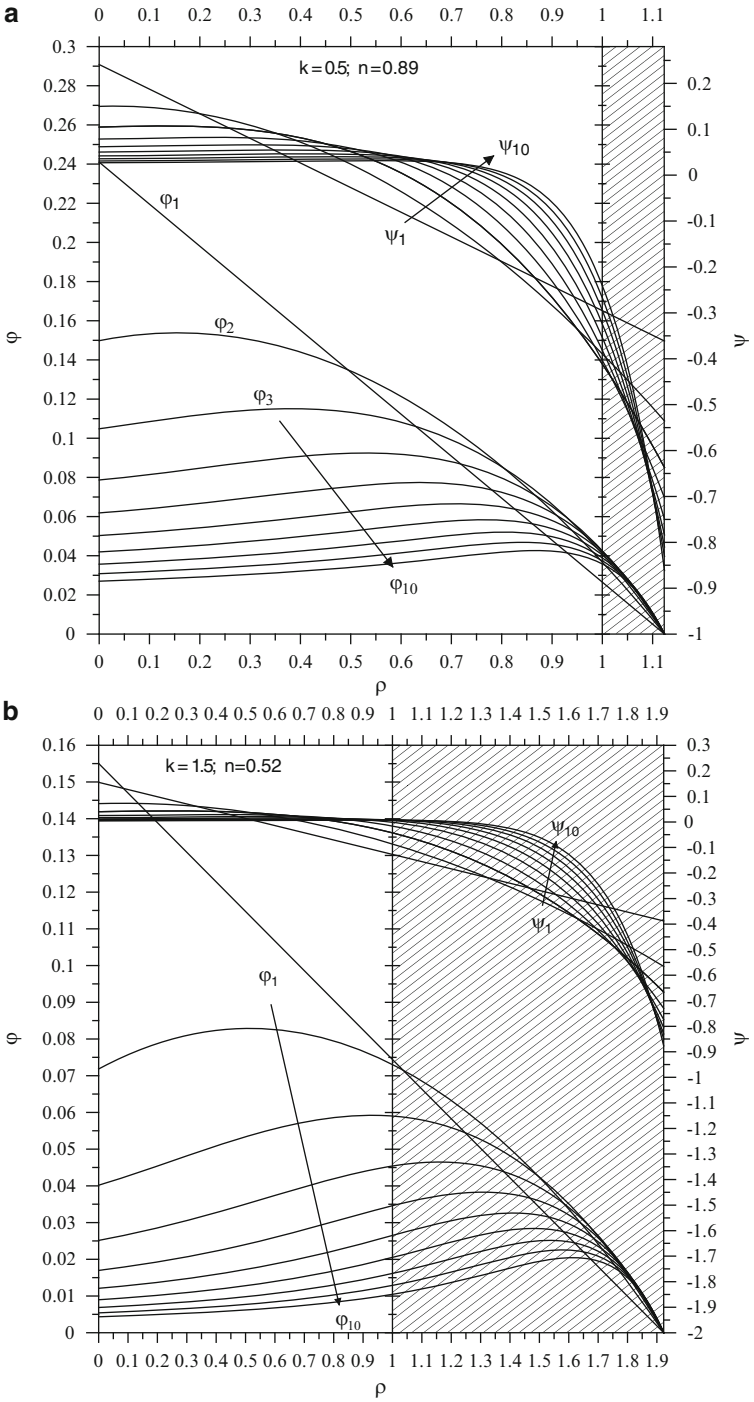

Fig. 7.7 Distribution of $\varphi_i(\rho)$ and $\psi_i(\rho)$, as functions of ρ, within the interval $0 \leq \rho \leq 1/n$, up to $i = 10$, for two steel disks ($\nu = 0.3$) having variable thickness according to (7.1): (**a**) convex profile ($k = 0.5$ and $n = 0.89$); (**b**) concave profile ($k = 1.5$ and $n = 0.52$)

in whose series γ_0 is the density of the rotor material, while $\gamma_1, \gamma_2, \ldots$ are constants, and $i = 1, 2, \ldots, n$. Function (7.39) is similar to (3.44), except that the dimensionless variable ρ takes the place of the radial coordinate r. Thus, by considering (7.39) and by applying it to solve differential equation (7.4), we obtain:

$$\frac{d^2u}{d\rho^2} + \left(\frac{1}{\rho} - \frac{n \cdot k}{1 - n \cdot \rho}\right) \cdot \frac{du}{d\rho} - \left[\frac{1}{\rho^2} + \frac{v \cdot n \cdot k}{\rho \cdot (1 - n \cdot \rho)}\right] \cdot u + \left(1 - v^2\right) \cdot \frac{\omega^2 \cdot r_e^3 \cdot \rho}{E} \cdot \sum_{i=0}^{n} \gamma_i \cdot \rho^i = 0. \tag{7.40}$$

In this case too, the general integral of (7.40) is the sum of the solution of the homogeneous equation, which is already known, and of a particular integral of the non-homogeneous equation. The latter can be obtained as the linear combination of contributions deriving from component n terms $\gamma_i \cdot \rho^i$ (with $i = 0, 1, 2, \ldots, n$) of the function $\gamma = \gamma\ (\rho)$; thus, by considering the *i-th* term of this function, (7.40) becomes:

$$\frac{d^2u}{d\rho^2} + \left(\frac{1}{\rho} - \frac{n \cdot k}{1 - n \cdot \rho}\right) \cdot \frac{du}{d\rho} - \left[\frac{1}{\rho^2} + \frac{v \cdot n \cdot k}{\rho \cdot (1 - n \cdot \rho)}\right] \cdot u + \left(1 - v^2\right) \cdot \frac{\omega^2 \cdot r_e^3}{E} \cdot \gamma_i \cdot \rho^{i+1} = 0. \tag{7.41}$$

Relation (7.41), with $i = 0$, can be used to calculate the displacement $u = u(\rho)$ related to density γ_0 of the non-linearly profile disk's basic material; the same equation, with $i = 1, 2, \ldots, n$, makes it possible to determine the contributions related to the fictitious variation of density along the radius deriving from radial blades on lateral surfaces.

The particular integrals of differential equation (7.41) can be obtained using the same procedure as that adopted for equations (7.26) and (7.27) governing thermal loading. For the sake of brevity, the analytical developments will not be specified here. Through these developments, the stress state for a non-linearly variable thickness disk with a fictitious density variation along its radius is expressed as the sum of the partial contributions of the particular integrals, and thus in the following form:

$$\begin{cases} \sigma_r = \omega^2 \cdot r_e^2 \cdot (\gamma_0 \cdot g_r + \gamma_1 \cdot \eta_1 + \gamma_2 \cdot \eta_2 + \ldots) \\ \sigma_t = \omega^2 \cdot r_e^2 \cdot (\gamma_0 \cdot g_t + \gamma_1 \cdot \zeta_1 + \gamma_2 \cdot \zeta_2 + \ldots), \end{cases} \tag{7.42}$$

where $g_r, g_t, \eta_1, \zeta_1, \eta_2, \zeta_2, \ldots$ are functions of t, v, k and n. Functions g_r and g_t related to the particular integral in (7.41) with $i = 0$ are obtained from relations (7.12).

In general terms, for any value of i, the relations whereby functions $\eta_i(\rho)$ and $\zeta_i(\rho)$ appearing in expressions (7.42) can be calculated are as follows:

$$\eta_i(\rho) = -\frac{(i+3+v)\cdot\rho^{i+2}}{(i+4)\cdot(i+2)+k\cdot(i+3+v)} + n^{-(i+2)}\cdot\frac{(i+3+v)\cdot\prod_{j=1}^{i+1}(j^2+2j)}{\prod_{j=1}^{i+2}[j^2+2j+k\cdot(1+j+v)]}$$
$$+(i+3+v)\cdot\sum_{m=1}^{i+1}\frac{(m+1+v)\cdot k\cdot\rho^m\cdot n^{m-i-2}\cdot\prod_{j=m+1}^{i+1}(j^2+2j)}{\prod_{j=m}^{i+2}[j^2+2j+k\cdot(1+j+v)]};$$

$$\zeta_i(\rho) = -\frac{[1+(i+3)\cdot v]\cdot\rho^{i+2}}{(i+4)\cdot(i+2)+k\cdot(i+3+v)} + n^{-(i+2)}\cdot\frac{(i+3+v)\cdot\prod_{j=1}^{i+1}(j^2+2j)}{\prod_{j=1}^{i+2}[j^2+2j+k\cdot(1+j+v)]}$$
$$+(i+3+v)\cdot\sum_{m=1}^{i+1}\frac{[1+(m+1)\cdot v]\cdot k\cdot\rho^m\cdot n^{m-i-2}\cdot\prod_{j=m+1}^{i+1}(j^2+2j)}{\prod_{j=m}^{i+2}[j^2+2j+k\cdot(1+j+v)]}. \tag{7.43}$$

These general relations, which were also derived by the authors [78], can be used to obtain several others of greater technical relevance for engineering calculations, viz.: $i = 1$, $i = 2$ and $i = 3$. Indeed, almost all functions $\gamma = \gamma\ (\rho)$ found in commonly used disks can be satisfactorily approximated with a third-order polynomial.

The explicit relations whereby $\eta_i(\rho)$ and $\zeta_i(\rho)$ can be calculated for $i = 1$ are as follows (explicit expressions of $\eta_2(\rho)$, $\zeta_2(\rho)$ and $\eta_3(\rho)$, $\zeta_3(\rho)$ are omitted because they are very long):

(a) For $i = 1$, $\gamma = \gamma_1\cdot\rho$ and, hence:

$$\eta_1(\rho) = \frac{(4+v)\cdot\{(3+v)\cdot[3+k\cdot(2+v)]\cdot k\cdot n^2\rho^2+8\cdot(2+v)\cdot k\cdot n\cdot\rho+24\}}{n^3\cdot[15+k\cdot(4+v)]\cdot[8+k\cdot(3+v)]\cdot[3+k\cdot(2+v)]}$$
$$-\frac{(4+v)\cdot\{[8+k\cdot(3+v)]\cdot[3+k\cdot(2+v)]\cdot n^3\rho^3\}}{n^3\cdot[15+k\cdot(4+v)]\cdot[8+k\cdot(3+v)]\cdot[3+k\cdot(2+v)]};$$
$$\zeta_1(\rho) = \frac{-(1+4v)\cdot[8+k\cdot(3+v)]\cdot[3+k\cdot(2+v)]\cdot n^3\rho^3}{n^3\cdot[15+k\cdot(4+v)]\cdot[8+k\cdot(3+v)]\cdot[3+k\cdot(2+v)]}$$
$$+\frac{(4+v)\cdot\{(1+3v)\cdot[3+k\cdot(2+v)]\cdot k\cdot n^2\rho^2+8\cdot(1+2v)\cdot k\cdot n\cdot\rho+24\}}{n^3\cdot[15+k\cdot(4+v)]\cdot[8+k\cdot(3+v)]\cdot[3+k\cdot(2+v)]} \tag{7.44}$$

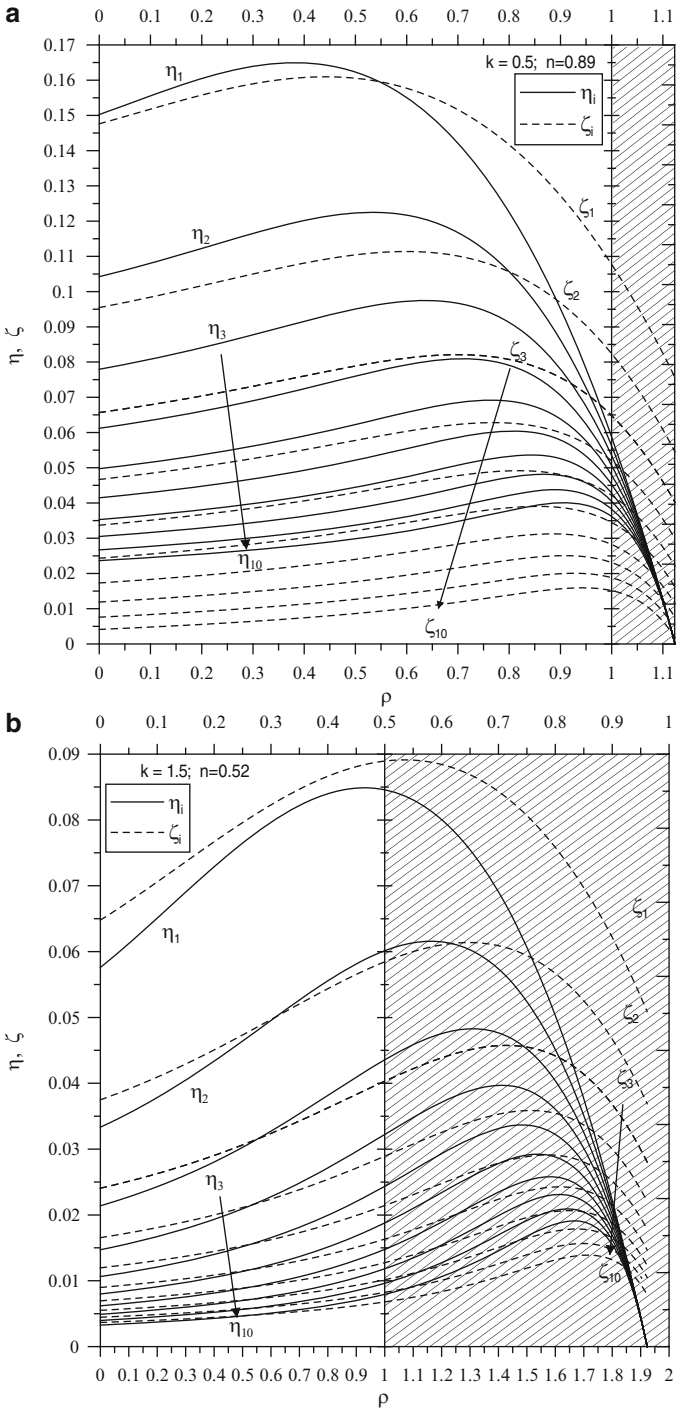

Fig. 7.8 Distribution of $\eta_i(\rho)$ and $\zeta_i(\rho)$, as functions of ρ, within the interval $0 \leq \rho \leq 1/n$, up to $i = 10$, for two steel disks ($\nu = 0.3$) having variable thickness according to (7.1): (**a**) convex profile ($k = 0.5$ and $n = 0.89$); (**b**) concave profile ($k = 1.5$ and $n = 0.52$)

Figure 7.8a, b show functions $\eta_i(\rho)$ and $\zeta_i(\rho)$ up to $i = 10$ versus dimensionless variable ρ for two steel disks ($v = 0.3$), one convex ($k = 0.5$ and $n = 0.89$), and the other concave ($k = 1.5$ and $n = 0.52$).

On the basis of (6.40), with $\sigma_0 = \gamma \cdot \omega^2 \cdot {r_e}^2$, and a_r, b_r, a_t and b_t given by (6.26), and (7.42), the stress state in a rotating disk having variable thickness according to a power of a linear function and featuring a fictitious density variation along the radius can be expressed as follows:

$$\begin{aligned}\sigma_r &= A \cdot a_r + B \cdot b_r + \omega^2 \cdot r_e^2 \cdot (\gamma_0 \cdot g_r + \gamma_1 \cdot \eta_1 + \gamma_2 \cdot \eta_2 + \gamma_3 \cdot \eta_3 + ...)\\ \sigma_t &= A \cdot a_t + B \cdot b_t + \omega^2 \cdot r_e^2 \cdot (\gamma_0 \cdot g_t + \gamma_1 \cdot \zeta_2 + \gamma_2 \cdot \zeta_2 + \gamma_3 \cdot \zeta_3 + ...).\end{aligned} \tag{7.45}$$

Here again, the strain state associated with the above stress state is obtained from (1.25) from which temperature terms are omitted, after substituting relations (7.45) in them; we will then have $u = r{\cdot}\varepsilon_t$.

Likewise, it should be noted that all of the above relations for density variation along the radius are generalizations of those obtained for the conical disk, which is thus a specific case of the variable-thickness disk according to (7.1). Written in terms of variable t, these relations can be used to obtain, for $n = k = 1$, relations for the converging conical disk, and for $n = -1$ and $k = 1$ relations for the diverging conical disk.

7.5 Non-Linearly Variable Thickness Disks with Density Variation and Subjected to Thermal and Centrifugal Loads

Lastly, we will consider a non-linearly variable thickness rotating disk subjected to thermal load and having density variation along its radius. It will be assumed that the functions $T = T(r)$ and $\gamma = \gamma(r)$ are the polynomials given by (4.5) and (7.39) respectively. Since the principle of superposition applies in the linear elastic field, it is obvious that, taking (7.31) and (7.38) into account, the stress state will be given by the relations:

$$\begin{cases}\sigma_r = A \cdot a_r + B \cdot b_r + \omega^2 \cdot r_e^2 \cdot (\gamma_0 \cdot g_r + \gamma_1 \cdot \eta_1 + \gamma_2 \cdot \eta_2 + \gamma_3 \cdot \eta_3 + ...)\\ \qquad + E \cdot \alpha \cdot \varphi(\rho)\\ \sigma_t = A \cdot a_t + B \cdot b_t + \omega^2 \cdot r_e^2 \cdot (\gamma_0 \cdot g_t + \gamma_1 \cdot \zeta_2 + \gamma_2 \cdot \zeta_2 + \gamma_3 \cdot \zeta_3 + ...)\\ \qquad + E \cdot \alpha \cdot \psi(\rho),\end{cases} \tag{7.46}$$

while the associated strain state will be given by (1.25) after substituting the above relations in them. Radial displacement, on the other hand, will be derived from the usual relation $u = r{\cdot}\varepsilon_t$.

7.6 Examples of Non-Linear Variable Thickness Disks

A number of numerical examples will be given below which illustrate how to proceed in calculating the stress and strain states in steel disks ($\nu = 0.3$; $E = 204$ GPa, $\gamma = 7{,}800$ kg/m^3, $\alpha = 12{\cdot}10^{-6}$ °C^{-1}) with thickness varying according to relation (7.1) and having profiles of interest for actual applications, with the exception of those discussed in Sects. 7.6.1 and 7.6.2, which are of conceptual interest: the first makes it possible to give physical meaning to the particular integral u_p.

Here again, the results for these examples are compared with those obtained using finite element models. All of the considerations presented in Sect. 6.6 apply in this connection.

7.6.1 Rotating Solid Disk with Apex Singularity and Having Constant Density

This type of disk, although of little technical interest because of its pointed tip at outer radius $r = r_e = R$ deserves attention inasmuch as it makes it possible to assign inherent physical significance to particular integral u_p, which directly represents radial displacement in the solid disk having non-linearly variable thickness, extended to its apex R. Indeed, as was indicated earlier, given that u_1 tends to infinity at the disk apex ($r = R$, $t = 1$), whereas u_2 tends to infinity at the disk axis ($r = 0, t = 0$), the constants appearing in (6.39) must be zero in order to have finite values for displacement u. In other words, it is necessary that $C_1 = C_2 = 0$.

In this connection, it should be pointed out that relation (7.8), expressing u_p as a third-order polynomial in r, and thus relations (7.12), expressing functions g_r and g_t, already fulfil the boundary conditions:

$$\begin{cases} \sigma_r = \sigma_t & \text{for } r = 0 \ (\rho = 0) \\ \sigma_r = 0 & \text{for } r = R \ (\rho = 1). \end{cases} \tag{7.47}$$

Figure 7.9a, b show stress-distribution curves σ_r and σ_t and displacement-distribution curve $u = u_p$ as functions of ρ in two solid steel disks ($\nu = 0.3$; $E = 204$ GPa, $\gamma = 7{,}800$ kg/m^3), extended to the apex radius $r_e = R$ ($R = 1$ m), both rotating at angular velocity $\omega = 314$ rad/s, the first showing a convex profile ($k = 0.5$ and $n = 1$), the second a concave profile ($k = 1.5$ and $n = 1$).

The figures indicate that: (1) the curves for σ_r and σ_t follow those for functions g_r and g_t, differing for σ_0; (2) stresses σ_r exceed stresses σ_t, locally though by a small amount; (3) the maximum stress values in the concave disk, which has less mass, are significantly below those occurring, all other conditions remaining equal, in the convex disk.

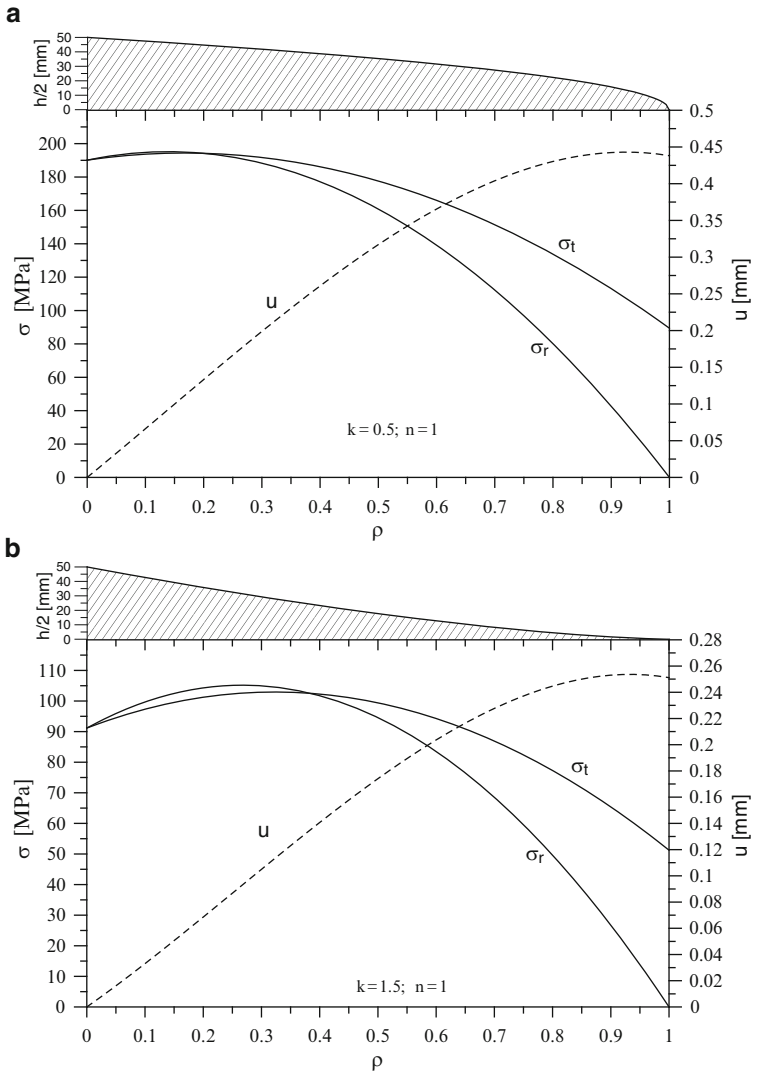

Fig. 7.9 Stress-distribution curves σ_r, σ_t and displacement-distribution curve $u = u_p$ in two solid rotating steel disks ($\nu = 0.3$) with profile variable according to (7.1) and featuring apex singularity and constant density: (**a**) convex profile ($k = 0.5$ and $n = 1$); (**b**) concave profile ($k = 1.5$ and $n = 1$)

7.6.2 Rotating Annular Disk with Apex Singularity and Having Constant Density

If the two rotating disks of the type considered in the preceding example are annular (this is another case of little design interest), the constant C_1 appearing in (6.39) must be zero in order to have a finite value for radial displacement u at the outer edge, where $r = R$ ($t = 1$); at the inner edge, given that the disks are annular, $t \neq 0$,

and we will thus have $C_2 \neq 0$, as there is no singularity correlated with u_2 for $t = 0$. The relation whereby the displacement field can be calculated in this case is (6.39) from which term u_1 is omitted. The two boundary conditions are as follows:

$$\begin{cases} \sigma_r = \sigma_{ri} & \text{for } r = r_i \ (\rho = \beta) \\ \sigma_r = 0 & \text{for } r = R \ (\rho = 1). \end{cases} \tag{7.48}$$

As was shown, the second boundary condition is already fulfilled by u_p and u_2, while integration constant C_2 is obtained from the first boundary condition. Supposing that $\sigma_{ri} = 0$, i.e., that the disk inner surfaces are not loaded, the value of constant C_2 is obtained by equalling to zero (for $r = r_i$) terms in square brackets appearing in the first of (1.27), from which temperature terms are omitted, and by introducing $u = C_2 \cdot u_2 + u_p$.

As this is a case of little design interest, the developments have little to add from the conceptual standpoint and will be left to the reader.

7.6.3 *Rotating Solid Disks with $r_e < R$ and Having Constant Density*

In this type of disk, as u_2 tends to infinity at the disk axis ($r = 0$, $\rho = 0$), constant C_2 appearing in (6.39) must be zero in order to obtain a finite value of radial displacement u at this radius. Moreover, given that the disk is of the frustum type ($r_e < R$), $\rho = 1 < 1/n$ at the disk outer radius, and as there is no u_1-related singularity for $\rho = 1/n$, then $C_1 \neq 0$. The relation whereby the displacement field can be calculated in this case is (6.39) from which term u_2 is omitted. The boundary conditions are as follows:

$$\begin{cases} \sigma_r = \sigma_t & \text{for } r = 0 \ (\rho = 0). \\ \sigma_r = \sigma_{re} & \text{for } r = r_e \ (\rho = 1). \end{cases} \tag{7.49}$$

The first boundary condition is already fulfilled by u_p and, as was shown, by u_1, while integration constant C_1 is obtained from the second boundary condition. Supposing that $\sigma_{re} = 0$, i.e., that the disk outer surface is not loaded, the value of constant C_1 is obtained by equalling to zero (for $r = r_e$) terms in square brackets appearing in the first of (1.27), from which temperature terms are omitted, and by introducing $u = C_1 \cdot u_1 + u_p$.

Figure 7.10a, b show stress-distribution curves σ_r and σ_t and displacement-distribution curve u as functions of ρ in two solid steel disks ($\nu = 0.3$; $E = 204$ GPa, $\gamma = 7{,}800$ kg/m^3), extended to outer radius $r_e = 0.8$ m, thickness at axis $h_0 = 0.1$ m and thickness at periphery $h_e = h_0/3$, no loaded at outer radius ($\sigma_{re} = 0$), both rotating at angular velocity $\omega = 314$ rad/s, though the first shows a convex profile ($k = 0.5$ and $q = 0.89$), and the second shows a concave profile

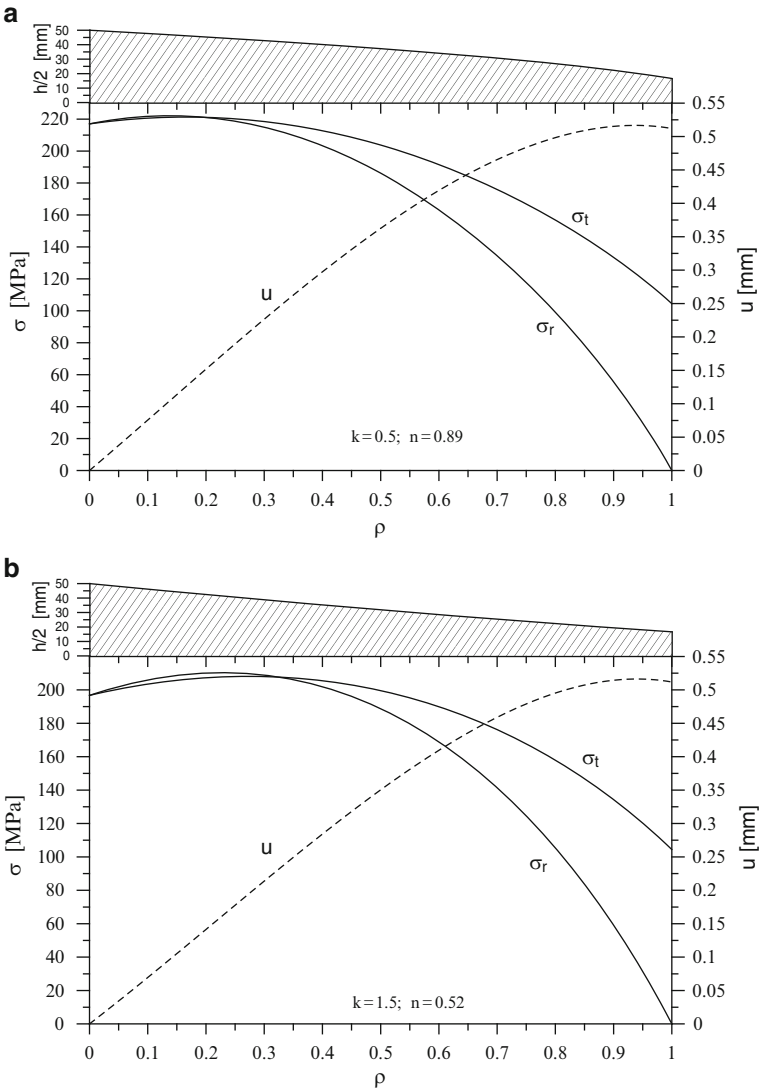

Fig. 7.10 Stress-distribution curves σ_r, σ_t and displacement-distribution curve u in two solid rotating steel disks ($\nu = 0.3$) having variable profile according to (7.1) with constant density and $r_e < R$: (**a**) convex profile ($k = 0.5$ and $n = 0.89$); (**b**) concave profile ($k = 1.5$ and n = 0.52)

($k = 1.5$ and $q = 0.52$). It is clear from a comparison of the two diagrams that, for actual disks featuring a finite thickness at the crown ring boundary (where $\rho = 1$), the differences between the concave and the convex profile are much less pronounced, and also that, as regards the stress state, the concave profile is slightly preferable to the convex profile.

7.6.4 Rotating Annular Disks with $r_e < R$ and Having Constant Density

As the majority of disks used in current machinery applications feature a central hole of inner radius $r_i > 0$ and an outer radius $r_e < R$, problems deriving from two singularity points $t = 0$ and $t = 1$ do not apply. In this case, radial displacement u is obtained from (6.39) complete with all terms. As there are no singularity points, it is advisable to calculate the stress field by using relations (6.40), determining integration constants A and B by establishing:

$$\begin{cases} \sigma_r = \sigma_{ri} & \text{for } \rho = \beta \\ \sigma_r = \sigma_{re} & \text{for } \rho = 1. \end{cases} \tag{7.50}$$

Constants C_1 and C_2 in (6.39) can be determined by using relations (7.25).

Figure 7.11a, b show stress-distribution curves σ_r and σ_t and displacement-distribution curve u as functions of ρ in two steel annular disks ($\nu = 0.3$) with $r_i = 0.1$ m, $r_e = 0.8$ m, $h_0 = 0.1$ m, and $h_e = h_0/3$, both rotating at angular velocity $\omega = 314$ rad/s and not loaded either at outer or inner radius ($\sigma_{ri} = 0$; $\sigma_{re} = 0$), the first showing a convex profile ($k = 0.5$ and $n = 0.89$), and the second a concave profile ($k = 1.5$ and $n = 0.52$). Here again, a comparison of the diagrams leads to the same conclusions reached in the preceding paragraph.

7.6.5 Rotating Disks with Hub and Crown Ring and Having Constant Density

If, as often occurs in machinery applications (Fig. 7.12), the disk features a crown ring and a hub, both of which are considered of constant thickness, it is first necessary to determine radial stresses $\sigma_{r,A}$ and $\sigma_{r,B}$ present in section A ($r = r_i$) and in section B ($r = r_e$) respectively, and which constitute two unknown hyperstatic values.

By imposing boundary conditions on the disk, constants A and B are first determined from the first of relations (6.40), and are expressed as functions of unknown values $\sigma_{r,A}$ and $\sigma_{r,B}$. Equations (6.40) are then used to obtain relations expressing σ_r and σ_t as functions of $\sigma_{r,A}$ and $\sigma_{r,B}$. Lastly, by imposing equality of radial displacements of the interface A, first regarded as a part of the disk and second as a part of the hub, and of the interface B, also regarded first as a part of the disk and second as a part of the crown ring, we determine unknown hyperstatic values $\sigma_{r,A}$ and $\sigma_{r,B}$ and, proceeding backwards, all other items (in this connection, see calculation example 3 of Sect. 2.5.3).

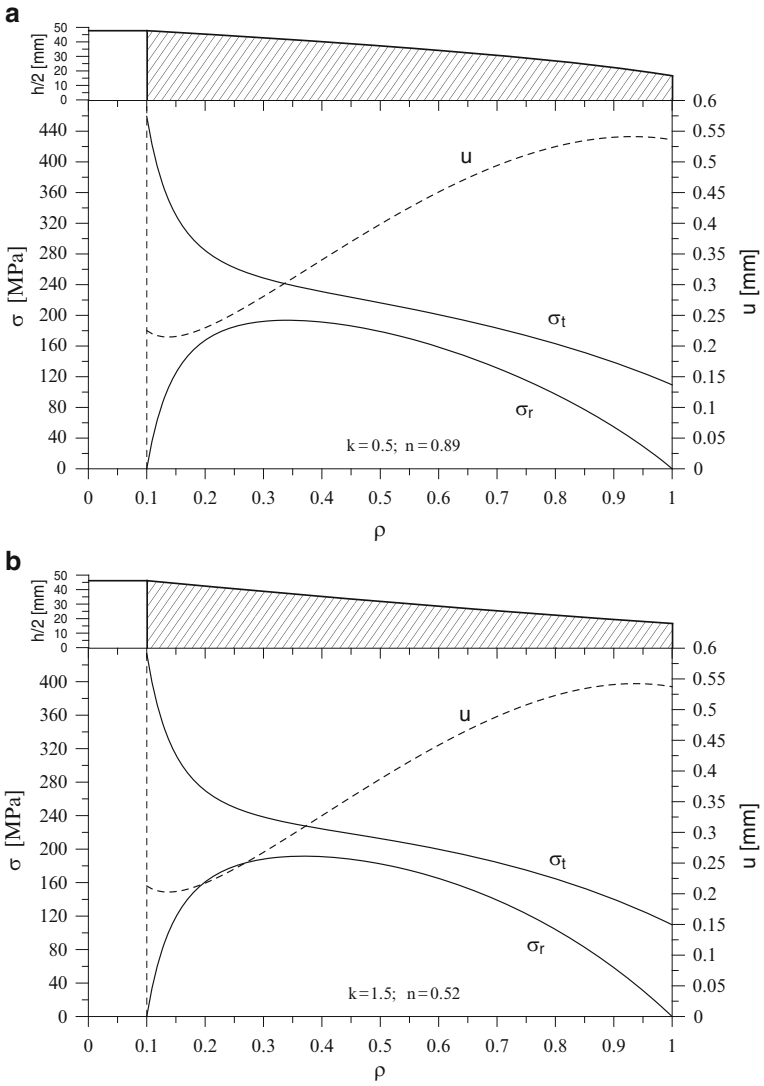

Fig. 7.11 Stress-distribution curves σ_r, σ_t and displacement-distribution curve u in two annular rotating steel disks ($\nu = 0.3$) having variable profile according to (7.1) with constant density: (**a**) convex profile ($k = 0.5$ and $n = 0.89$); (**b**) concave profile ($k = 1.5$ and $n = 0.52$)

It should be noted that, by appropriately selecting the disk profile, along with crown ring and hub, stresses σ_r and σ_t can be made almost constant; in other words, a disk of uniform strength can be approximated within certain limits.

In the practical examples in Fig. 7.12a, b, the crown ring is simulated by a radial stress at interface $B(\sigma_{rB} = 120$ MPa), while the hub may assume three configurations which differ in mass. For each of these configurations, the

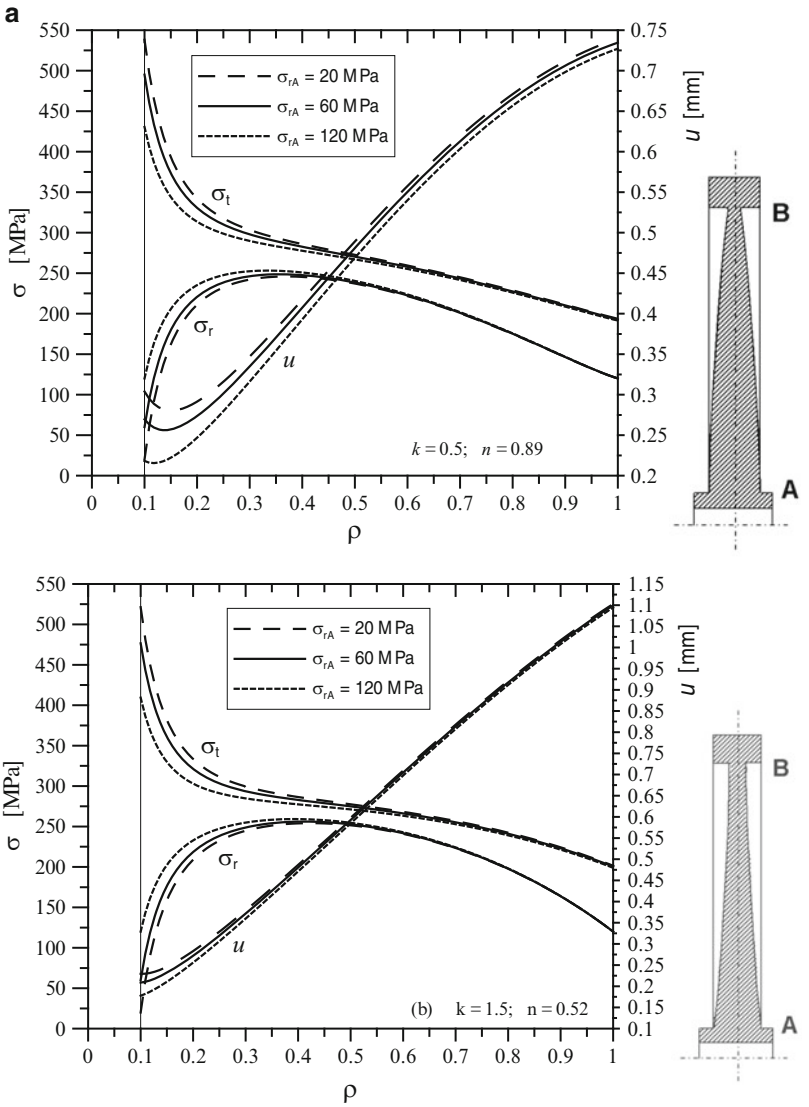

Fig. 7.12 Stress-distribution curves σ_r, σ_t and displacement-distribution curve u in two steel disks ($\nu = 0.3$) having variable thickness according to (7.1), with hub and crown ring, for three different hub configurations, each showing a specific interface stress distribution $\sigma_{r,A}$: (**a**) convex profile ($k = 0.5$ and $n = 0.89$); (**b**) concave profile ($k = 1.5$ and $n = 0.52$)

corresponding interface stresses $\sigma_{r,A}$ are indicated, but not the geometry. Figure 7.12a, b show stress-distribution curves σ_r and σ_t and displacement-distribution curve u as functions of ρ for two disks, the first showing a convex profile ($k = 0.5$ and $n = 0.89$), and the second a concave profile ($k = 1.5$ and $n = 0.52$), clarifying that the most advantageous stress distribution is obtained with the hub having greater mass.

7.6.6 Annular Disks Having Constant Density and Subjected to Temperature Gradient

We will now examine two non-linearly variable thickness disks which, like those analysed in Sect. 7.6.4, are of constant density and have no singularity points. Here, however, the disks are not rotating and are subjected to thermal load only, with temperature varying according to relation (4.5), with $i = 3$. In this case, the stress state is obtained from relations (7.38), while integration constants A and B are determined by imposing boundary conditions (7.50) of Sect. 7.6.4.

Figure 7.13a, b show stress-distribution curves σ_r and σ_t and displacement-distribution curve u as functions of ρ in two annular disks, featuring the same geometry and made of the same material ($\nu = 0.3$ and $\alpha = 12{\cdot}10^{-6}\ {}^{\circ}\mathrm{C}^{-1}$) as the ones examined in Sect. 7.6.4, not loaded at either inner or outer edge and subjected to a temperature gradient along the radius according to function $T = T_0 + k_1 r + k_2 r^2 + k_3 r^3$. The same figure shows curves of the temperature distribution, T being dimensionless relative to reference temperature T_0, as well as coefficients of the third-order polynomial function. A comparison of the diagrams shows no substantial differences between the concave and convex profile disks.

7.6.7 Rotating Annular Disks Having Density Variation on Radius

We will now examine two rotating disks which, like those analysed in Sect. 7.6.4, have no singularity points, are not subjected to thermal load, and have variable density along the radius according to relation (7.39), with $i = 3$. Here, however, the stress state is obtained from relations (7.42), while integration constants A and B are determined by imposing boundary conditions (7.50).

Figure 7.14a, b show stress-distribution curves σ_r and σ_t and displacement-distribution curve u as functions of ρ in the two annular steel disks ($\nu = 0.3$) featuring the same geometry and made of the same material as the ones examined in Sect. 7.6.4, rotating at angular velocity $\omega = 314$ rad/s, not loaded at either inner or outer edge, but featuring variable density along the radius according to function $\gamma = \gamma_0 + \gamma_1 \cdot \rho + \gamma_2 \cdot \rho^2 + \gamma_3 \cdot \rho^3$. The same figure shows the curve of the density variation, γ being dimensionless relative to the basic material density γ_0, as well as coefficients of the third-order polynomial function.

A comparison of the diagrams shows minor differences between the concave and the convex profile disk.

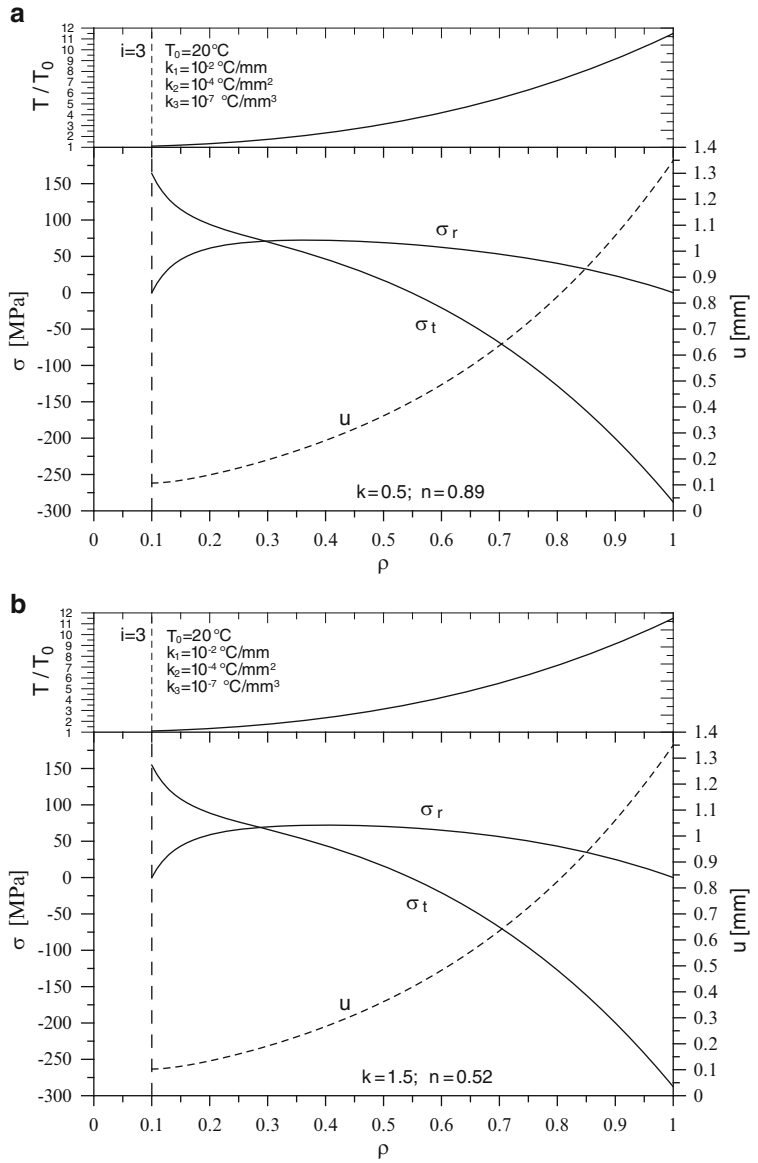

Fig. 7.13 Stress-distribution curves σ_r, σ_t and displacement-distribution curve u in two steel disks ($v = 0.3$) having variable thickness according to (7.1), subjected to thermal gradient only: (**a**) convex profile ($k = 0.5$ and $n = 0.89$); (**b**) concave profile ($k = 1.5$ and $n = 0.52$)

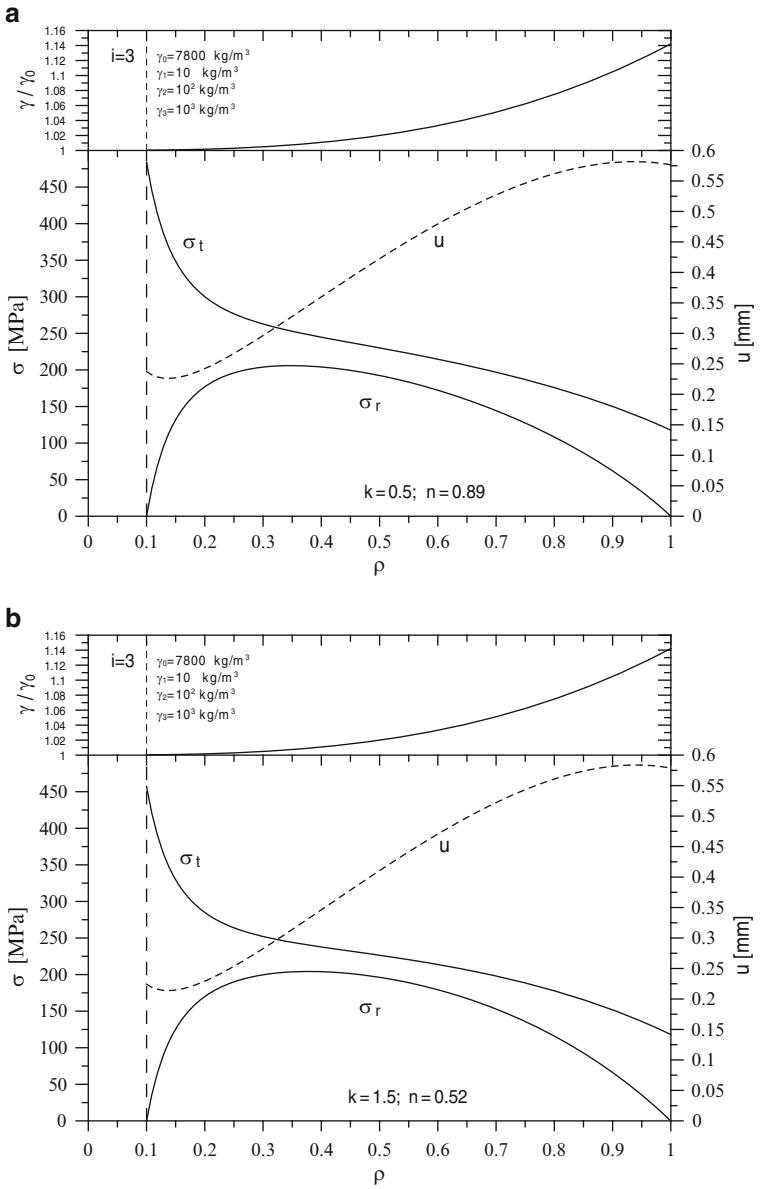

Fig. 7.14 Stress-distribution curves σ_r, σ_t and displacement-distribution curve u in two annular steel disks ($\nu = 0.3$) having variable thickness according to (7.1), showing variable density along the radius: (**a**) convex profile ($k = 0.5$ and $n = 0.89$); (**b**) concave profile ($k = 1.5$ and $n = 0.52$)

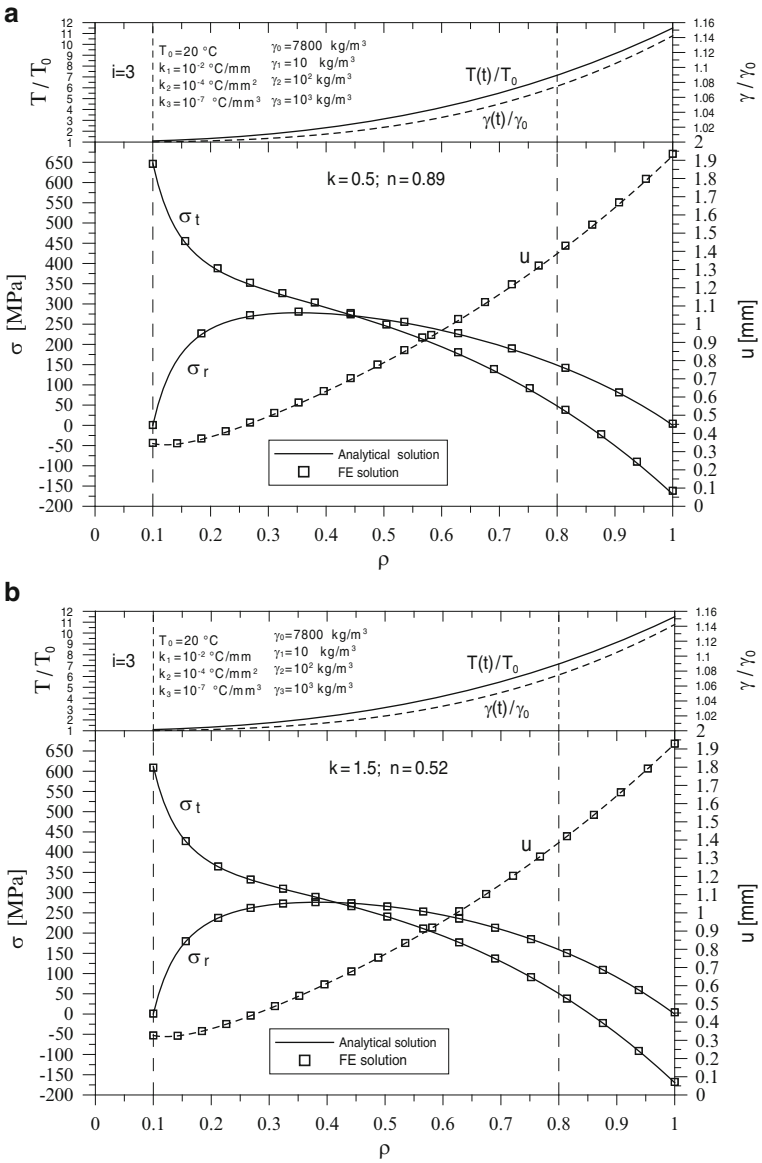

Fig. 7.15 Stress-distribution curves σ_r, σ_t and displacement-distribution curve u in two annular steel disks ($\nu = 0.3$) having variable thickness according to (7.1), subjected to thermal gradient and showing variable density along the radius, and comparison with FE-obtained results: (**a**) convex profile ($k = 0.5$ and $n = 0.89$); (**b**) concave profile ($k = 1.5$ and $n = 0.52$)

7.6.8 Rotating Annular Disks Having Density Variation on Radius and Subjected to Thermal Load

Here, the same disks featured in the previous two examples will be examined, but rotating and subjected to thermal load, with temperature varying according to relation (4.5), with $i = 3$, and having variable density along the radius according to expression (7.39), still with $i = 3$. In this case, the stress state is obtained from relations (7.46), while integration constants A and B are determined by imposing boundary conditions (7.50).

Figure 7.15a, b show stress-distribution curves σ_r and σ_t and displacement-distribution curve u as functions of ρ in the two annular steel disks ($\nu = 0.3$) featuring the same geometry and made of the same material as the ones examined in the previous two examples, not loaded at either inner or outer edge, subject to a temperature gradient along the radius and featuring variable density along the radius. The functions of variation for T and γ are the cubical ones referred to in the two preceding examples, and shown in the diagram in dimensionless form. A comparison of the diagrams shows minor differences between the concave and the convex profile disks.

The figure also compares the results obtained by applying the analytical method proposed here and the numerical results obtained, all other conditions remaining unchanged, through FEM. The diagrams clearly show that the results of the numerical model and those of the analytical model match perfectly.

7.6.9 Comparing Various Disk Types

Four solid disk configurations will now be compared *ceteris paribus*, respectively with conical ($k = 1$ and $n = 0.67$), convex ($k = 0.5$ and $n = 0.89$) and concave ($k = 1.5$ and $n = 0.52$) profiles and the fourth with uniform strength profile. All four rotating disks are subjected to a stress distribution σ_{re} at the outer radius r_e.

All four disks taken into consideration fall into the category discussed in Sect. 7.6.3. Accordingly, the conditions indicated in said section also apply here, the only variation being $\sigma_r = \sigma_{re} \neq 0$ at the outer radius r_e. By imposing this boundary condition and bearing in mind that $C_2 = B = 0$ and $u = C_1 u_1 + u_p$, the value of constant A will be obtained from the first of relations (6.40) and, consequently, the value of the constant C_1 will be obtained from the first of relations (7.25).

Figure 7.16 shows the profile geometries, as well as curves of stress-distribution curves σ_r/σ_{re}, σ_t/σ_{re} and displacement-distribution curve u/u_0 as functions of ρ in the four solid disks. Stress values are dimensionless relative to stress value σ_{re}, whereas displacement values are dimensionless relative to $u_0 = r_e\, \sigma_{re}\, (1 - \nu)/E$.

Comparison of these diagrams shows that the convex profile most closely matches the stress state of the uniform-strength disk, whereas the concave profile features the

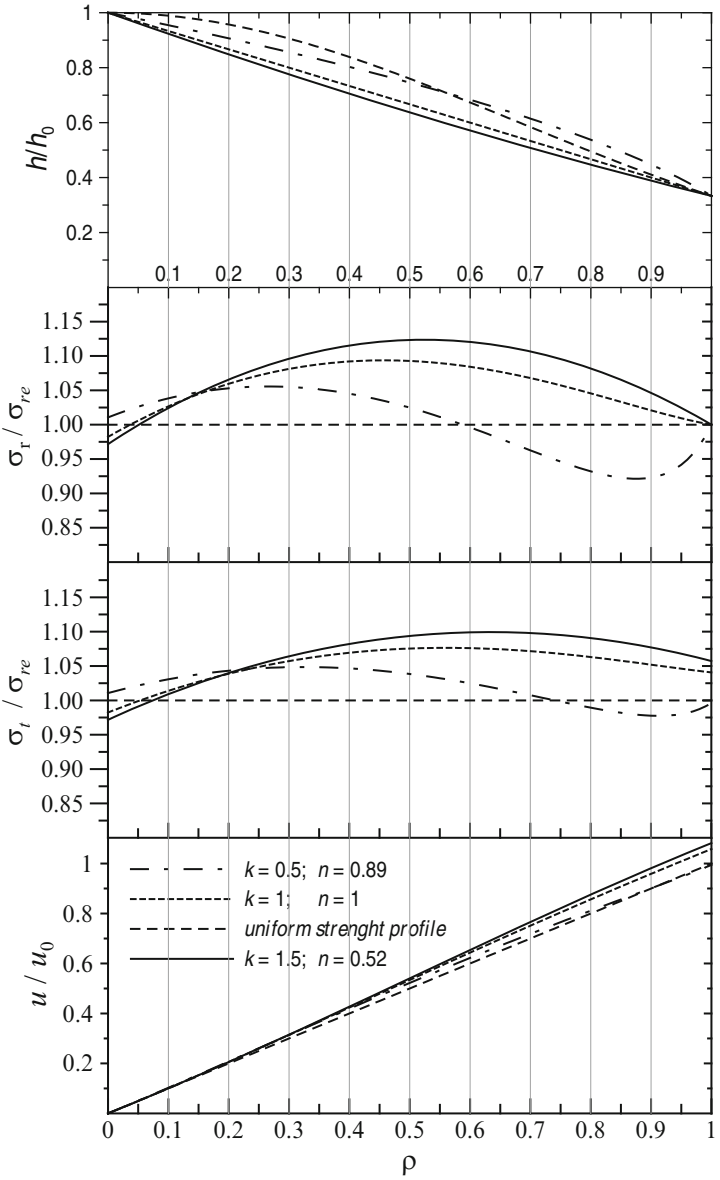

Fig. 7.16 Comparison of four solid, variable-profile disks. From the top: profile geometries; σ_r/σ_{re} versus ρ; σ_t/σ_{re} versus ρ; u/u_0 versus ρ

most substantial discrepancies. Behaviour of the conical profile is midway between that of the concave and the convex profiles. As regards radial displacement, there are no differences of design significance between the four profiles.

7.7 Non-Linearly Variable Thickness Disks Subjected to Angular Acceleration

If the disk has a thickness that varies according to a power of a linear function expressed by relation (7.1) and is subjected to angular acceleration, the solution does not involve difficulties comparable to those encountered above in analysing equilibrium and compatibility in the radial direction. In this case, the solution of (2.74) is as follows:

$$\tau_{rt} = \dot{\omega} r_e^2 \gamma \frac{(n\rho - 1)}{\rho^2 n^4} \times \frac{[\rho^3 n^3 (k+3)(k+2)(k+1) + 3\rho^2 n^2 (k+2)(k+1) + 6\rho n(k+1) + 6]}{(k+4)(k+3)(k+2)(k+1)} + \frac{C}{\rho^2 (n\rho - 1)^k}, \tag{7.51}$$

where C is an integration constant that can be determined by establishing that the shear stress at the outer radius assumes the value $(\tau_{rt})_e$, deriving from the application of a driving or braking torque at the rim of the disk. By setting this boundary condition, we obtain the relation:

$$\tau_{rt} = \frac{\gamma \dot{\omega} r_e^2}{\rho^2 n^4} \cdot \frac{(n\rho - 1)}{(k+4)\cdot(k+3)\cdot(k+2)\cdot(k+1)} \times \left\{ \left[\rho^3 n^3 (k+3)\cdot(k+2)\cdot(k+1) + 3\rho^2 n^2 (k+2)\cdot(k+1) + 6\rho n \cdot (k+1) + 6\right] + \right. + \frac{(n-1)^{k+1}}{(n\rho - 1)^{k+1}} \left[n^3 (k+3)\cdot(k+2)\cdot(k+1) + 3n^2 (k+2)\cdot(k+1) + 6n\cdot(k+1) + 6\right] + + \left. \frac{(n-1)^k}{(n\rho - 1)^{k+1}} \cdot \frac{(\tau_{rt})_e}{\gamma \cdot \dot{\omega} \cdot r_e^2} \cdot n^4 (k+4)\cdot(k+3)\cdot(k+2)\cdot(k+1) \right\}. \tag{7.52}$$

If no driving or braking torque is applied at the outer radius of a constant density disk whose thickness varies according to (7.1), relation (7.51) gives $C = 0$. Consequently, as $(\tau_{rt})_e = 0$, we will have:

$$\tau_{rt} = \frac{\gamma \dot{\omega} r_e^2}{\rho^2 n^4} \cdot \frac{(n\rho - 1)}{(k+4)\cdot(k+3)\cdot(k+2)\cdot(k+1)} \times \left\{ \left[\rho^3 n^3 (k+3)\cdot(k+2)\cdot(k+1) + 3\rho^2 n^2 (k+2)\cdot(k+1) + 6\rho n \cdot (k+1) + 6\right] + + \frac{(n-1)^{k+1}}{(n\rho - 1)^{k+1}} \left[n^3 (k+3)\cdot(k+2)\cdot(k+1) + 3n^2 (k+2)\cdot(k+1) + 6n\cdot(k+1) + 6\right] \right\}. \tag{7.53}$$

It is obvious that if we set $k = 1$, the above relations give the shear stress resulting from angular acceleration in a conical disk whose profile varies along with parameter n, as shown in Fig. 7.1a.